

Alkynyl-diphenylphosphine d⁸ (Pt, Rh, Ir) Complexes: Contrasting Behavior toward *cis*-[Pt(C₆F₅)₂(THF)₂]Jesús R. Berenguer,[†] María Bernechea,[†] Juan Fornies,^{*‡} Ana García,[†] Elena Lalinde,^{*†} and M. Teresa Moreno[†]

Departamento de Química-Grupo de Síntesis Química de La Rioja, UA-CSIC, Universidad de La Rioja, 26006, Logroño, Spain, and Departamento de Química Inorgánica, Instituto de Ciencia de Materiales de Aragón, Universidad de Zaragoza-Consejo Superior de Investigaciones Científicas, 50009 Zaragoza, Spain

Received July 27, 2004

The synthesis and characterization of a series of mononuclear d⁸ complexes with at least two P-coordinated alkynylphosphine ligands and their reactivity toward *cis*-[Pt(C₆F₅)₂(THF)₂] are reported. The cationic [Pt(C₆F₅)(PPh₂C≡CPh)₃](CF₃SO₃), **1**, [M(COD)(PPh₂C≡CPh)₂](ClO₄) (M = Rh, **2**, and Ir, **3**), and neutral [Pt(*o*-C₆H₄E₂)(PPh₂C≡CPh)₂] (E = O, **6**, and S, **7**) complexes have been prepared, and the crystal structures of **1**, **2**, and **7**·CH₃COCH₃ have been determined by X-ray crystallography. The course of the reactions of the mononuclear complexes **1–3**, **6**, and **7** with *cis*-[Pt(C₆F₅)₂(THF)₂] is strongly influenced by the metal and the ligands. Thus, treatment of **1** with 1 equiv of *cis*-[Pt(C₆F₅)₂(THF)₂] gives the double inserted cationic product [Pt(C₆F₅)(S)μ-{C(Ph)=C(PPh₂)C(PPh₂)=C(Ph)(C₆F₅)}Pt(C₆F₅)(PPh₂C≡CPh)](CF₃SO₃) (S = THF, H₂O), **8** (S = H₂O, X-ray), which evolves in solution to the mononuclear complex [(C₆F₅)(PPh₂C≡CPh)Pt{C₁₀H₄-1-C₆F₅-4-Ph-2,3-κ^{PP}(PPh₂)₂}] (CF₃SO₃), **9** (X-ray), containing a 1-pentafluorophenyl-2,3-bis(diphenylphosphine)-4-phenylnaphthalene ligand, formed by annulation of a phenyl group and loss of the Pt(C₆F₅) unit. However, analogous reactions using **2** or **3** as precursors afford mixtures of complexes, from which we have characterized by X-ray crystallography the alkynylphosphine oxide compound [(C₆F₅)₂Pt(μ-κ^O:η²-PPh₂O)C≡CPh]₂, **10**, in the reaction with the iridium complex (**3**). Complexes **6** and **7**, which contain additional potential bridging donor atoms (O, S), react with *cis*-[Pt(C₆F₅)₂(THF)₂] in the appropriate molar ratio (1:1 or 1:2) to give homo- bi- or trinuclear [Pt(PPh₂C≡CPh)(μ-κ^E-*o*-C₆H₄E₂)(μ-κ^P:η²-PPh₂C≡CPh)Pt(C₆F₅)₂] (E = O, **11**, and S, **12**) and [Pt(μ₃-κ²EE'-*o*-C₆H₄E₂)(μ-κ^P:η²-PPh₂C≡CPh)₂]{Pt(C₆F₅)₂} (E = O, **13**, and S, **14**) complexes. The molecular structure of **14** has been confirmed by X-ray diffraction, and the cyclic voltammetric behavior of precursor complexes **6** and **7** and polynuclear derivatives **11–14** has been examined.

Introduction

This work is part of our systematic investigation into alkynylphosphine–transition metal complexes. Alkynylphosphines PPh₂C≡CR are polyfunctional ligands which show versatile behavior in coordination chemistry. Their interest is due to different factors including (i) the ability of alkynylphosphine ligands to adopt various coordination modes,^{1–15} (ii) the facility with which these ligands undergo

P–C(alkyne) bond cleavage processes, generating acetylide (C≡C) and phosphide (PPh₂) fragments,^{16–21} which are frequently involved in subsequent coupling or insertion reactions,^{22–26} (iii) the possibility of a variety of interesting ligand-based couplings^{27,28} and insertion reactions,^{29–36} and (iv) the possible activation of the uncoordinated alkynyl function upon simple P-coordination toward nucleophilic or electrophilic attacks.^{28,37–39}

* Authors to whom correspondence should be addressed. E-mail: elena.lalinde@dq.unirioja.es (E.L.), forniesj@posta.unizar.es (J.F.).

[†] Universidad de La Rioja, UA-CSIC.

[‡] Universidad de Zaragoza-CSIC.

(1) Went, M. J. *Polyhedron* **1995**, *14*, 465.

(2) Baumgartner, T.; Huynh, K.; Schleidt, S.; Lough, A. J.; Manners, I. *Chem.–Eur. J.* **2002**, *8*, 4622.

(3) Louattani, E.; Suades, J. *J. Organomet. Chem.* **2000**, *604*, 234.

(4) Bardají, M.; Laguna, A.; Jones, P. G. *Organometallics* **2001**, *20*, 3906.

(5) Louattani, E.; Suades, J. *Inorg. Chim. Acta* **1999**, *291*, 207.

(6) Lucas, N. T.; Cifuentes, M. P.; Nguyen, L. T.; Humphrey, M. G. *J. Cluster Sci.* **2001**, *12*, 201.

(7) Patel, H. A.; Carty, A. J.; Hota, N. K. *J. Organomet. Chem.* **1973**, *50*, 247.

Several years ago, Carty and co-workers showed that diphenyl(phenylethynyl)phosphine complexes *cis*-[MX(Y)-(PPh₂C≡CPh)₂] [X = Y = Cl, I, CF₃, C₆F₅; X(Y) = *o*-C₆H₄O₂, Me(Cl)] suffer intramolecular coupling of the alkynylphosphine ligands on heating to form the bis-(diphenylphosphino)naphthalene complexes *cis*-[PtX(Y)-{*o*-C₁₆H₁₀(PPh₂)₂}].^{27,28} With the aim of investigating the possibility of inducing the alkyne coupling of two P-coordinated PPh₂C≡CR ligands by η²-coordination to a second metal center, we decided to examine the reactivity of *cis*-[MX₂(PPh₂C≡CR)₂] (M = Pt, Pd; X = Cl, C≡CR', C₆F₅) toward the platinum or palladium species *cis*-[M(C₆F₅)₂(THF)₂] (M = Pt, Pd; THF = tetrahydrofuran). These reactions strongly depend on the nature of the X and R groups. Thus, when X is a group which has a tendency to

form bridges between metal centers, it competes with the η²-bonding capability of the PPh₂C≡CR groups to coordinate the “*cis*-M(C₆F₅)₂” fragments.^{40,41} However, when X is a group with low tendency to form bridges, we have found an unusual reactivity pattern. Thus, *cis*-[M(C₆F₅)₂(PPh₂C≡CR)₂] (M = Pt, Pd; R = Ph, Tol) react with *cis*-[Pt(C₆F₅)₂(THF)₂] to give unusual μ-2,3-bis(diphenylphosphino)-1,3-butadienyl binuclear complexes {μ-C(R)=C(PPh₂)C(PPh₂)=C(R)-C₆F₅} formed from initial bis(η²-alkyne) adducts (μ-κP:η²-PPh₂C≡CR)₂ (detected at low temperature) through an unexpectedly easy sequential insertion of both PPh₂C≡CR into a robust Pt–C₆F₅ bond.^{42,43} The overall process is regio- and stereoselective leading, in the case of *cis*-[Pt(C₆F₅)₂(PPh₂C≡CR)(PPh₂C≡C*t*Bu)], to a very crowded butadienyl C(*t*Bu)=C(PPh₂)C(PPh₂)=C(C₆F₅)R backbone, which stabilizes an unprecedented, T-shaped, unsaturated three-coordinated platinum center in solid state (R = Tol). In this context and to study the different factors (metal, charge, and coligands) that influence the course of this insertion process, we considered it of interest to prepare novel d⁸ cationic or neutral complexes stabilized by at least two P-coordinated PPh₂C≡CPh ligands and to study their reactivity toward *cis*-[Pt(C₆F₅)₂(THF)₂]. In this paper we report the synthesis of novel cationic [Pt(C₆F₅)(PPh₂C≡CPh)₃](CF₃SO₃) and [M(COD)(PPh₂C≡CPh)₂](ClO₄) (M = Rh, Ir) and neutral [Pt(*o*-C₆H₄S₂)(PPh₂C≡CPh)₂] derivatives and the results of their reactions and those of the analogous catecholate complex [Pt(*o*-C₆H₄O₂)(PPh₂C≡CPh)₂],²⁸ **6**, with *cis*-[Pt(C₆F₅)₂(THF)₂].

Experimental Section

General Considerations. All reactions and manipulations were carried out under nitrogen atmosphere using Schlenk techniques and distilled solvents purified by known procedures. IR spectra were recorded on a Perkin-Elmer FT-IR 1000 spectrometer as Nujol mulls between polyethylene sheets. NMR spectra were recorded on a Bruker ARX 300 spectrometer; chemical shifts are reported in ppm relative to external standards (SiMe₄, CFC₁₃, and 85% H₃PO₄), and coupling constants, in Hz. Elemental analyses were carried out with a Perkin-Elmer 2400 CHNS/O microanalyzer, and the electro spray mass spectra, on a HP5989B with interphase API-ES HP 59987A. Conductivities were measured in acetone solutions (ca. 5 × 10⁻⁴ mol L⁻¹) using a Crison GLP31 conductimeter. Cyclic voltammetric studies were performed using an EG&G-283 potentiostat/galvanostat. A standard three-electrode configuration was used, with platinum working and platinum auxiliary electrodes and a saturated calomel electrode (SCE reference). All potentials are quoted vs the ferrocene/ferrocenium couple (Fc/Fc⁺) (used as an internal reference). Anhydrous CH₂Cl₂ was used as solvent under a nitrogen atmosphere, and 0.1 M (NBu₄)(PF₆) was used as supporting electrolyte. PPh₂C≡CPh,⁴⁴ [Pt(μ-Cl)(C₆F₅)(tht)]₂,⁴⁵ [M(μ-Cl)-

- (8) Bennett, M. A.; Castro, J.; Edwards, A. J.; Kopp, M. R.; Wenger, E.; Willis, A. C. *Organometallics* **2001**, *20*, 980.
 (9) Bennett, M. A.; Kwan, L.; Rae, A. D.; Wenger, E.; Willis, A. C. *J. Chem. Soc., Dalton Trans.* **2002**, 226.
 (10) Carty, A. J.; Dimock, K.; Paik, H. N.; Palenik, G. J. *J. Organomet. Chem.* **1974**, *70*, C17.
 (11) Carty, A. J.; Smith, W. F.; Taylor, N. J. *J. Organomet. Chem.* **1978**, *146*, C1.
 (12) Carty, A. J.; Paik, H. N.; Palenik, G. J. *Inorg. Chem.* **1977**, *16*, 300.
 (13) Sappa, E.; Predieri, G.; Tiripicchio, A.; Tiripicchio-Camellini, M. *J. Organomet. Chem.* **1985**, *297*, 103.
 (14) Louattani, E.; Suades, J.; Alvarez-Larena, A.; Piniella, F.; Germain, G. *J. Organomet. Chem.* **1996**, *506*, 121.
 (15) Berenguer, J. R.; Bernechea, M.; Forniés, J.; Gómez, J.; Lalinde, E. *Organometallics* **2002**, *21*, 2314.
 (16) Carty, A. J. *Pure Appl. Chem.* **1982**, *54*, 113 and references therein.
 (17) Carty, A. J.; Taylor, N. J.; Smith, W. F. *J. Chem. Soc., Chem. Commun.* **1979**, 750.
 (18) Bruce, M. I.; Williams, M. L.; Patrick, J. M.; White, A. H. *J. Chem. Soc., Dalton Trans.* **1985**, 1229.
 (19) Nuccianore, D.; MacLaughlin, S. A.; Taylor, N. J.; Carty, A. J. *Organometallics* **1988**, *7*, 106.
 (20) Cherkas, A. A.; Randall, L. H.; MacLaughlin, S. A.; Mott, G. N.; Taylor, N. J.; Carty, A. J. *Organometallics* **1988**, *7*, 969.
 (21) Hogarth, G.; Rechmond, S. P. *J. Organomet. Chem.* **1997**, *534*, 221.
 (22) Sappa, E.; Pasquinelli, A.; Tiripicchio, A.; Tiripicchio-Camellini, M. *J. Chem. Soc., Dalton Trans.* **1989**, 601.
 (23) Benvenuti, M. H.; Vargas, M. D.; Braga, D.; Crepioni, F.; Mann, B. E.; Taylor, S. *Organometallics* **1993**, *12*, 2947.
 (24) Pereira, R. M. S.; Fujiwara, F. Y.; Vargas, M. D.; Braga, D.; Crepioni, F. *Organometallics* **1997**, *16*, 4833.
 (25) Delgado, E.; Chi, Y.; Wang, W.; Hogarth, G.; Low, P. J.; Enright, G. D.; Peng, S.-M.; Lee, G.-H. *Organometallics* **1998**, *17*, 2936.
 (26) Davies, J. E.; Mays, M. J.; Raithby, P. R.; Sarveswaran, K.; Solan, G. A. *J. Chem. Soc., Dalton Trans.* **2001**, 1269.
 (27) Carty, A. J.; Taylor, N. J.; Johnson, D. K. *J. Am. Chem. Soc.* **1979**, *101*, 5422.
 (28) Johnson, D. K.; Rukachaisirikul, T.; Sun, Y.; Taylor, N. J.; Carty, A. J.; Carty, A. J. *Inorg. Chem.* **1993**, *32*, 5544.
 (29) Montlo, D.; Suades, J.; Dahan, F.; Mathieu, R. *Organometallics* **1990**, *9*, 2933.
 (30) Liu, X.; Lukehart, C. M. *Organometallics* **1992**, *11*, 3993.
 (31) Dupuis, L.; Pirió, N.; Meunier, P.; Igau, A.; Donnadiéu, D.; Mayoral, J.-P. *Angew. Chem., Int. Ed. Engl.* **1997**, *36*, 987.
 (32) Rosa, P.; Le Floch, P.; Ricard, L.; Mathey, F. *J. Am. Chem. Soc.* **1997**, *119*, 9417.
 (33) Miquel, Y.; Igau, A.; Donnadiéu, B.; Mayoral, J. P.; Pirió, N.; Meunier, P. *J. Am. Chem. Soc.* **1998**, *120*, 3504.
 (34) Miquel, Y.; Cadierno, V.; Donnadiéu, B.; Igau, A.; Mayoral, J.-P. *Organometallics* **2000**, *19*, 54.
 (35) Bennett, M. A.; Cobley, C. J.; Rae, A. D.; Wenger, E.; Willis, A. C. *Organometallics* **2000**, *19*, 1522.
 (36) Edwards, A. J.; Macgregor, S. A.; Rae, A. D.; Wenger, E.; Willis, A. C. *Organometallics* **2001**, *20*, 2864.
 (37) Carty, A. J.; Jacobson, S.; Simpson, R. T.; Taylor, N. J. *J. Am. Chem. Soc.* **1975**, *97*, 7254.
 (38) Carty, A. J.; Johnson, D. K.; Jacobson, S. *J. Am. Chem. Soc.* **1979**, *101*, 5612.
 (39) Taylor, N. J.; Jacobson, S.; Carty, A. J. *Inorg. Chem.* **1975**, *14*, 2648.

- (40) Forniés, J.; Lalinde, E.; Martín, A.; Moreno, M. T.; Welch, A. J. *J. Chem. Soc., Dalton Trans.* **1995**, 1333.
 (41) Ara, I.; Falvello, L. R.; Fernández, S.; Forniés, J.; Lalinde, E.; Martín, A.; Moreno, M. T. *Organometallics* **1997**, *16*, 5923.
 (42) Charmant, J. P. H.; Forniés, J.; Gómez, J.; Lalinde, E.; Moreno, M. T.; Orpen, A. G.; Solano, S. *Angew. Chem., Int. Ed.* **1999**, *38*, 3058.
 (43) Ara, I.; Forniés, J.; García, A.; Gómez, J.; Lalinde, E.; Moreno, M. T. *Chem.—Eur. J.* **2002**, *8*, 3698.
 (44) Carty, A. J.; Hota, N. K.; Ng, T. W.; Patel, H. A.; O'Connor, T. J. *Can. J. Chem.* **1971**, *49*, 2706.

(COD)]₂ (M = Rh,⁴⁶ Ir⁴⁷), *cis*-[PtCl₂(DMSO)₂]₂,⁴⁸ *cis*-[Pt(C₆F₅)₂(THF)]₂,⁴⁹ and PPh₂(O)C≡CPh⁵⁰ were prepared according to literature methods.

Safety Note. Perchlorate salts with organic ligands are potentially explosive. Only small amounts of material should be prepared, and these should be handled with great caution.

Synthesis of [Pt(C₆F₅)(PPh₂C≡CPh)₃](CF₃SO₃), **1.** A yellow solution of [Pt(μ -Cl)(C₆F₅)(tht)]₂ (0.120 g, 0.123 mmol) in acetone (40 mL) was treated with AgCF₃SO₃ (0.0635 g, 0.247 mmol) and the mixture stirred for 1 h at room temperature and then filtered through Kieselgurh. To the resulting yellow solution was added PPh₂C≡CPh (0.212 g, 0.741 mmol), and the mixture was stirred for 1 h. Evaporation to dryness and treatment with EtOH (5 mL) afforded **1** as a white solid (0.223 g, 66% yield). Anal. Calcd for C₆₇F₈H₄₅O₃P₃PtS (M_r = 1370.15): C, 58.73; H, 3.31; S, 2.34. Found: C, 58.64; H, 3.10; S, 2.30. Λ_M : 122 $\Omega^{-1}\cdot\text{cm}^2\cdot\text{mol}^{-1}$. MS ES (+): m/z 1220 ([M - TfO]⁺, 27%), 935 ([M - TfO - PPh₂C≡CPh]⁺, 11%), 766 ([Pt(PPh₂C≡CPh)₂]⁺, 36%). IR (cm⁻¹): $\nu(\text{C}\equiv\text{C})$ 2171 vs; $\nu(\text{C}_6\text{F}_5)_{\text{Xsens}}$ 793 s; $\nu(\text{CF}_3\text{SO}_3)$ 1271 s, 1222 m, 1159 s, 1030 m. ¹H NMR (CDCl₃, 20 °C, δ): 7.70 (m, 5H), 7.41 (m, 12 H), 7.28 (m, 22H), 7.00 (d, 4H), 6.78 (d, 2H), Ph. ¹⁹F NMR (CDCl₃, 20 °C, δ): -78.2 (s, 3F, CF₃), -117.3 [dd, ³J(Pt-F_o) = 262.6 Hz, 2F_o], -158.9 (t, 1F_p), -160.5 (m, 2F_m). ³¹P{¹H} NMR (CDCl₃, 20 °C, δ): -6.3 [d, 2P, ¹J(P-P)_{cis} = 20 Hz, ¹J(P-Pt) = 2607 Hz], -7.5 [m, br, P trans to C₆F₅, ¹J(P-Pt) = 2339 Hz]. ¹³C{¹H} NMR (CDCl₃, 20 °C, δ): 145.1–133.5 (C₆F₅), 134.0 [d, ²J(C-P) = 12.6 Hz, C_o, PPh₂], 132.4–118.5 (PPh₂, Ph), 111.5 [AXX', ²J(C-P) + ⁴J(C-P) = 19.7 Hz, C _{β} , PPh₂C _{α} ≡C _{β} Ph cis to C₆F₅], 109.9 [d, ²J(C-P) = 16.1 Hz, C _{β} , PPh₂C≡CPh trans to C₆F₅], 80.5 [dt, ¹J(C-P) = 108.7 Hz, ³J(C-P) = 5.3 Hz, C _{α} , PPh₂C≡CPh trans to C₆F₅], 77.9 [dd, ¹J(C-P) + ³J(C-P) = 63.5 Hz, C _{α} , PPh₂C≡CPh cis to C₆F₅].

Synthesis of [Rh(COD)(PPh₂C≡CPh)₂](ClO₄), **2.** A yellow solution of [Rh(μ -Cl)(COD)]₂ (0.500 g, 1.014 mmol) in acetone (20 mL) was treated with AgClO₄ (0.420 g, 2.028 mmol). The mixture was stirred for 1 h at room temperature and filtered through Kieselgurh, and the resulting yellow filtrate was treated with PPh₂C≡CPh (1.161 g, 4.056 mmol). Immediately the brown-orange solution obtained was evaporated to small volume (2 mL). By addition of diethyl ether (10 mL) and cooling at -20 °C, an orange microcrystalline solid (**2**) was obtained (1.220 g, 68% yield). Anal. Calcd for C₄₈ClH₄₂O₄P₂Rh (M_r = 883.17): C, 65.28; H, 4.79. Found: C, 64.96; H, 4.64. Λ_M : 116 $\Omega^{-1}\cdot\text{cm}^2\cdot\text{mol}^{-1}$. MS ES (+): m/z 783 ([M - ClO₄]⁺, 100%). IR (cm⁻¹): $\nu(\text{C}\equiv\text{C})$ 2177 s; $\nu(\text{ClO}_4^-)$ 1092 vs, 623 m. ¹H NMR (CDCl₃, 20 °C, δ): 7.67 (m, 8H), 7.40 (m, 12 H), 7.21 (m, 6H), 7.03 (m, 4H) Ph, 4.85 (s, br, 4H, CH=, COD), 2.55 (m, br, 4H, CH₂<, COD), 2.41 (m, br, 4H, CH₂<, COD). ³¹P{¹H} NMR (CDCl₃, 20 °C, δ): 8.25 [d, ¹J(P-Rh) = 150.1 Hz]. ¹³C{¹H} NMR (CDCl₃, 20 °C, δ): 133.4 [“t”, ²J(C-P) + ⁴J(C-P) = 13.3 Hz, C_o, PPh₂], 131.9 (s, C_o, ≡CPh), 131.6 (s, br, C_p, PPh₂), 130.4 (s, C_p, ≡CPh), 129.6 [AXX', ¹J(C-P) + ³J(C-P) = 55.2 Hz, C_i, PPh₂], 129.2 [“t”, ³J(C-P) + ⁵J(C-P) = 11.2 Hz, C_m, PPh₂], 128.4 (s, C_m, ≡CPh), 120.1 (s, C_i, ≡CPh), 109.1 [“t”, ²J(C-P) + ⁴J(C-P) = 14.3 Hz, C _{β}], 101.8 [dt, ¹J(C _{α} -Rh) ~ 1 Hz, ²J(C-P)_{cis} = 4.9 Hz, ²J(C-P)_{trans} = 7.3 Hz, CH=,

COD], 80.8 [AMXX', ¹J(C-P) + ³J(C-P) = 95.9 Hz, ²J(C _{α} -Rh) ~ 1 Hz, C _{α}], 30.7 (s CH₂<, COD).

Synthesis of [Ir(COD)(PPh₂C≡CPh)₂](ClO₄), **3.** A suspension of [Ir(μ -Cl)(COD)]₂ (0.100 g, 0.149 mmol) in acetone (20 mL) was treated with NaClO₄ (0.837 g, 5.96 mmol) and PPh₂C≡CPh (0.171 g, 0.556 mmol) (molar ratio 1:40:4). The color of the resulting suspension changed from orange to red, and the mixture was stirred for 1 h. The solvent was evaporated and the residue treated with CH₂Cl₂ (40 mL). After filtration through Kieselgurh, the filtrate was evaporated to dryness and the residue treated with diethyl ether (10 mL) affording a pink solid (**3**) (0.263 g, 91% yield). Anal. Calcd for C₄₈ClH₄₂O₄P₂Ir (M_r = 972.48): C, 59.28; H, 4.35. Found: C, 59.17; H, 4.52. Λ_M : 122 $\Omega^{-1}\cdot\text{cm}^2\cdot\text{mol}^{-1}$. MS ES (+): m/z 873 ([M - ClO₄]⁺, 100%). IR (cm⁻¹): $\nu(\text{C}\equiv\text{C})$ 2175 s; $\nu(\text{ClO}_4^-)$ 1094 vs, 623 m. ¹H NMR (CDCl₃, 20 °C, δ): 7.63 (m, 8H), 7.40 (m, 12 H), 7.22 (m, 6H), 7.03 (m, 4H) Ph, 4.50 (s, br, 4H, CH=, COD), 2.38 (m, br, 4H, CH₂<, COD), 2.22 (m, br, 4H, CH₂<, COD). ³¹P{¹H} NMR (CDCl₃, 20 °C, δ): -0.41 (s). ¹³C{¹H} NMR (CDCl₃, 20 °C, δ): 133.6 [“t”, ²J(C-P) + ⁴J(C-P) = 12.6 Hz; C_o, PPh₂], 132.1 (s, br, C_o, ≡CPh), 131.9 (s, C_p, PPh₂), 130.6 (s, C_p, ≡CPh), 129.0 [AXX', ¹J(C-P) + ³J(C-P) = 63.9 Hz, C_i, PPh₂], 129.1 [“t”, ³J(C-P) + ⁵J(C-P) = 11.6 Hz, C_m, PPh₂], 128.4 (s, C_m, ≡CPh), 119.8 (s, C_i, ≡CPh), 109.0 [AXX', ²J(C-P) + ⁴J(C-P) = 16.1 Hz, C _{β}], 90.2 [st, ¹J(C-P) = 11.7 Hz, CH=, COD], 80.2 [AXX', ¹J(C-P) + ³J(C-P) = 107.2 Hz, C _{α}], 31.3 (s, CH₂<, COD).

Synthesis of [Pt(*o*-C₆H₄O₂)(DMSO)₂], **4.** To a solution of potassium catecholate prepared by the treatment of catechol (0.078 g, 0.708 mmol) and potassium hydroxide (0.0795 g, 1.417 mmol) in methanol (10 mL) was added *cis*-[PtCl₂(DMSO)₂]₂ (0.299 g, 0.708 mmol) at room temperature. The initial grayish suspension became yellow in a few minutes. The mixture was stirred for 4 h, and the resulting suspension (complex **4**) was filtered as a yellow solid (0.304 g, 93% yield). Anal. Calcd for C₁₀H₁₆O₄PtS₂ (M_r = 459.4): C, 26.14; H, 3.51; S, 13.96. Found: C, 26.03; H, 3.42; S, 13.41. MS ES (+): m/z 764 ([Pt₂(C₆H₄O₂)₂(DMSO)₂]⁺, 13%), 460 ([M]⁺, 100%). IR (cm⁻¹): $\nu(\text{S}=\text{O})$ 1144 vs, 1134 vs. ¹H NMR (CDCl₃, 20 °C, δ): 6.69 (m, 2H), 6.59 (m, 2 H) (C₆H₄), 3.53 [s, 12H, CH₃, ³J(H-Pt) = 17.2 Hz]. ¹³C{¹H} NMR (CDCl₃, 20 °C, δ): 160.3 [s, C¹(O), C₆H₄O₂], 118.1 (s, C³, C₆H₄O₂), 115.6 [³J(Pt-C) = 52 Hz, C², C₆H₄O₂], 44.39 [²J(Pt-C) = 41.2 Hz, SO(CH₃)₂].

Synthesis of [Pt(*o*-C₆H₄S₂)(DMSO)₂], **5.** *cis*-[PtCl₂(DMSO)₂]₂ (1.017 g, 2.408 mmol) was added to a solution of potassium benzene-1,2-dithiolate (2.649 mmol) prepared with benzene-1,2-dithiol (300 μ L, 2.649 mmol) and potassium hydroxide (0.297 g, 5.298 mmol) in methanol (10 mL) at room temperature. The initial yellow suspension turned dark gray in a few minutes. After 4 h of stirring, **5** was filtered off as a very dark gray solid (1.124 g, 95% yield). Anal. Calcd for C₁₀H₁₆O₂PtS₄ (M_r = 491.57): C, 24.43; H, 3.28; S, 26.09. Found: C, 24.33; H, 2.56; S, 25.46. MS ES (+, Na⁺): m/z 1968 ([4M + 2]⁺, 100%), 1007 ([2M + Na]⁺, 17%), 515 ([M + Na]⁺, 60%). IR (cm⁻¹): $\nu(\text{S}=\text{O})$ 1157 s, 1126 s. ¹H NMR (HDA, 20 °C, δ): 7.30 (m, 2H), 6.83 (m, 2 H) (C₆H₄), 3.60 [s, 12H, CH₃, ³J(H-Pt) = 17.3 Hz]. Its low solubility precluded its characterization by ¹³C{¹H} NMR spectroscopy.

Synthesis of [Pt(*o*-C₆H₄O₂)(PPh₂C≡CPh)₂], **6.**²⁸ The synthesis of this complex has been previously reported, but we found a straightforward preparation from **4**. A yellow suspension of [Pt(*o*-C₆H₄O₂)(DMSO)₂], **4** (0.200 g, 0.436 mmol), in CH₂Cl₂ (20 mL) was treated with PPh₂C≡CPh (0.262 g, 0.915 mmol), to give an orange solution. After 2 h of stirring, the solution was filtered and evaporated to dryness, and the residue was treated with a mixture of 1:1 diethyl ether/*n*-hexane (6 mL), to give a pale-orange solid.

(45) Usón, R.; Forniés, J.; Espinet, P.; Alfranca, G. *Synth. React. Inorg. Met. Org. Chem.* **1980**, *10*, 579.

(46) Giordano, G.; Crabtree, R. H. *Inorg. Synth.* **1990**, *28*, 88.

(47) Herde, J. L.; Lambert, J. C.; Senoff, C. V. *Inorg. Synth.* **1974**, *15*, 18.

(48) Kitching, W.; Moore, C. J.; Doddrell, D. *Inorg. Chem.* **1970**, *9*, 541.

(49) Usón, R.; Forniés, J.; Tomás, M.; Menjón, B. *Organometallics* **1985**, *4*, 1912.

(50) Charrier, C.; Chodkiewicz, W.; Cadiot, P. *Bull. Soc. Chim. Fr.* **1966**, 1002.

This solid was recrystallized from CH_2Cl_2 /diethyl ether to afford **6** as an orange solid (0.253 g, 66% yield).

$^{13}\text{C}\{^1\text{H}\}$ NMR (CDCl_3 , 20 °C, δ): 162.9 [t, $^1J(\text{C}-\text{P}) + ^3J(\text{C}-\text{P}) = 3$ Hz, $\text{C}^1(\text{O})$, $\text{C}_6\text{H}_4\text{O}_2$], 133.6 [t, AXX' , $^2J(\text{C}-\text{P}) + ^4J(\text{C}-\text{P}) = 12.8$ Hz, C_o , PPh_2], 132.2 (s, C_o , $\equiv\text{CPh}$), 131.1 (s, C_p , PPh_2), 130.3 (s, C_p , Ph), 128.9 [AXX', five line pattern, $^1J(\text{C}-\text{P}) + ^3J(\text{C}-\text{P}) = 59.7$ Hz, C_i , PPh_2], 128.3 (m, C_m , PPh_2 , $\text{C}_m \equiv\text{CPh}$), 120.5 [t, $J(\text{C}-\text{P}) = 1.5$ Hz, C_i , $\equiv\text{CPh}$], 116.2 (s, C^3 , $\text{C}_6\text{H}_4\text{O}_2$), 115.4 [t, $J(\text{C}-\text{P}) = 1.5$ Hz, $^3J(\text{C}-\text{Pt}) = 58.6$ Hz, C^2 , $\text{C}_6\text{H}_4\text{O}_2$], 109.0 [AXX', $^2J(\text{C}-\text{P}) + ^4J(\text{C}-\text{P}) = 18.2$ Hz, C_β , $\equiv\text{C}_\beta\text{Ph}$], 79.0 [AXX', $^1J(\text{C}-\text{P}) + ^3J(\text{C}-\text{P}) = 120.2$ Hz, C_α , $\text{C}_\alpha \equiv$].

Synthesis of $[\text{Pt}(o\text{-C}_6\text{H}_4\text{S}_2)(\text{PPh}_2\text{C}\equiv\text{CPh})_2]$, **7.** A 0.460 g (1.608 mmol) amount of $\text{PPh}_2\text{C}\equiv\text{CPh}$ was added to a black suspension of $[\text{Pt}(o\text{-C}_6\text{H}_4\text{S}_2)(\text{DMSO})_2]$ (**5**) (0.395 g, 0.804 mmol) in CH_2Cl_2 (20 mL), and the mixture was stirred for 2 h. The resulting black solution was evaporated to dryness and the residue treated with diethyl ether (20 mL) to yield a gray solid (0.615 g, 84% yield). Crystallization at room temperature in aerobic conditions from an acetone solution gave yellow crystals, containing solvated acetone $7\text{-CH}_3\text{COCH}_3$, suitable for X-ray diffraction. ^1H and ^{31}P NMR spectra of both samples (gray solid and yellow crystals) are essentially identical except for the presence of coordinated acetone in the crystals. Anal. Calcd for $\text{C}_{46}\text{H}_{34}\text{P}_2\text{PtS}_2\text{-CH}_3\text{COCH}_3$ ($M_r = 966.01$): C, 60.92; H, 4.17; S, 6.64. Found: C, 60.51; H, 3.97; S, 6.56. MS ES (+): m/z 908 ($[\text{M}]^+$, 100%). IR (cm^{-1}): $\nu(\text{C}\equiv\text{C})$ 2176 vs. ^1H NMR (yellow crystals, CDCl_3 , 20 °C, δ): 7.82 (m, 8H), 7.33 (m), 7.17 (t), 6.98 (d, 24H), 6.70 (m, 2H), Ph, C_6H_4 , 2.16 (CH_3). $^{31}\text{P}\{^1\text{H}\}$ NMR (CDCl_3 , 20 °C, δ): -4.7 [s, $^1J(\text{Pt}-\text{P}) = 2909$ Hz]. $^{13}\text{C}\{^1\text{H}\}$ NMR (CDCl_3 , 20 °C, δ): 207.0 (C=O, acetone), 145.8 [AXX', $^1J(\text{C}-\text{P}) + ^3J(\text{C}-\text{P}) = 15.6$ Hz, $\text{C}^1\text{-S}$, $\text{C}_6\text{H}_4\text{S}_2$], 133.9 [AXX', five line pattern $^2J(\text{C}-\text{P}) + ^4J(\text{C}-\text{P}) = 12.8$ Hz, C_o , PPh_2], 132.2 (s, C_o , Ph), 131.0 (s, C_p , PPh_2), 130.1 [AXX', five line pattern, $^1J(\text{C}-\text{P}) + ^3J(\text{C}-\text{P}) = 67.8$ Hz, C_o , PPh_2], 130.0 (s, C_p , Ph), 128.2 [t, $J(\text{C}-\text{P}) \sim 0.5$ Hz, $^3J(\text{C}-\text{Pt}) \sim 67$ Hz, C^2 , $\text{C}_6\text{H}_4\text{S}_2$], 128.2 (t, C_m , PPh_2 , C_m Ph), 121.5 (s, br, C^3 , $\text{C}_6\text{H}_4\text{S}_2$), 120.8 [t, $J(\text{C}-\text{P}) \sim 1$ Hz, C_i , $\equiv\text{CPh}$], 108.0 [AXX', $^2J(\text{C}-\text{P}) + ^4J(\text{C}-\text{P}) = 16.3$ Hz, C_β , $\equiv\text{C}_\beta\text{Ph}$], 81.1 [d, $J(\text{C}-\text{P}) = 111.5$ Hz, C_α , $\text{C}_\alpha \equiv$], 31.0 (s, CH_3 , acetone).

Synthesis of $[\text{Pt}(\text{C}_6\text{F}_5)(\text{OH}_2)\mu\text{-}\{\text{C}(\text{Ph})=\text{C}(\text{PPh}_2)\text{C}(\text{PPh}_2)=\text{C}(\text{Ph})(\text{C}_6\text{F}_5)\}\text{Pt}(\text{C}_6\text{F}_5)(\text{PPh}_2\text{C}\equiv\text{CPh})](\text{CF}_3\text{SO}_3)$, **8.** *cis*- $[\text{Pt}(\text{C}_6\text{F}_5)_2(\text{THF})_2]$ (0.074 g, 0.110 mmol) was added to a colorless solution of $[\text{Pt}(\text{C}_6\text{F}_5)(\text{PPh}_2\text{C}\equiv\text{CPh})_3](\text{CF}_3\text{SO}_3)$, **1** (0.150 g, 0.110 mmol), in CH_2Cl_2 (15 mL) at room temperature, immediately forming an orange solution. After being stirred for 10 min, the solution was evaporated to small volume (2 mL). The addition of *n*-hexane (10 mL) gave **8** as an orange solid (0.139 g, 67% yield). Anal. Calcd for $\text{C}_{79}\text{F}_{18}\text{H}_{45}\text{O}_3\text{P}_3\text{PtS}\cdot 0.5\text{H}_2\text{O}\cdot 0.5\text{THF}$ ($M_r = 1944.42$): C, 50.04; H, 2.59; S, 1.65. Found: C, 49.99; H, 2.55; S, 1.36. Λ_M : 118 $\Omega^{-1}\text{cm}^2\text{mol}^{-1}$. MS ES (+): m/z 1750 ($[\text{M} - \text{TfO}]^+$, 100%), 1582 ($[\text{M} - \text{TfO} - \text{C}_6\text{F}_5]^+$, 17%), 1387 ($[\text{M} - \text{TfO} - \text{Pt}(\text{C}_6\text{F}_5)]^+$, 38%). IR (cm^{-1}): $\nu(\text{OH})$ 3604 w; $\nu(\text{C}\equiv\text{C})$ 2175 vs; $\nu(\text{C}_6\text{F}_5)$ 1519 vs, 1504 s, 1063 s, 980 s, 959 vs, 804 m, 799 m; $\nu(\text{CF}_3\text{SO}_3)$ 1293 (s), 1232 (m), 1161 (s), 1030 (s). ^1H NMR (CDCl_3 , 20 °C, δ): 9.17 (m, 2H), 7.98 (m, 4H), 7.71–6.43 (m, 35H), 6.10 (br, 2H), 5.35 (d, $J = 7.1$ Hz) (aromatics), 3.71 (s, br, OCH_2 , THF), 1.82 (s, br, CH_2 , THF), 1.70 (s, H_2O). ^{19}F NMR (CDCl_3 , 20 °C, δ): -78.4 (s, 3F, CF_3), -113.9 [m, $^3J(\text{Pt}-\text{F}_o) = 230$ Hz, 2F_o], -115.6 [m, $^3J(\text{Pt}-\text{F}_o) \sim 225$ Hz, 2F_o], -122.1 (m, br, 1F_{oA}), -133.3 [d, $^4J(\text{Pt}-\text{F}_o) \sim 75$ Hz, 1F_{oA}], -153.3 (br, 1F_{pA}), -158.8 (t, 1F_p), -159.1 (t, 1F_p), -160.3 (m, br, 2F_m), -161.6 (m, 1F_m), -162.5 (m, 1F_m), -164.1 (m, br, 2F_m). $^{31}\text{P}\{^1\text{H}\}$ NMR (CDCl_3 , 20 °C, δ): 32.4 [s, br, $^1J(\text{P}^2-\text{Pt}) = 2214$ Hz, P^2 trans to C_6F_5], 28.2 [dd, $^1J(\text{P}^3-\text{Pt}) = 2428$ Hz, $^2J(\text{P}^3-\text{Pt}) = 530$ Hz, $J(\text{P}^3-\text{P}^1)_{\text{trans}} = 362$ Hz, $^1J(\text{P}^3-$

$\text{P}^2)_{\text{cis}} = 14.3$ Hz, P^3], -5.9 [dd, $^1J(\text{P}^1-\text{Pt}) = 2486$ Hz, $J(\text{P}^1-\text{P}^3)_{\text{trans}} = 362$ Hz, $^1J(\text{P}^1-\text{P}^2)_{\text{cis}} = 14$ Hz, P^1].

Synthesis of $[(\text{C}_6\text{F}_5)(\text{PPh}_2\text{C}\equiv\text{CPh})\text{Pt}\{\text{C}_{10}\text{H}_4\text{-1-C}_6\text{F}_5\text{-4-Ph-2,3-}\kappa\text{PP}'(\text{PPh}_2)_2\}](\text{CF}_3\text{SO}_3)$, **9.** *cis*- $[\text{Pt}(\text{C}_6\text{F}_5)_2(\text{THF})_2]$ (0.081 g, 0.120 mmol) was added to a stirred solution of $[\text{Pt}(\text{C}_6\text{F}_5)(\text{PPh}_2\text{C}\equiv\text{CPh})_3](\text{CF}_3\text{SO}_3)$ (0.164 g, 0.120 mmol) in CH_2Cl_2 (15 mL) at room temperature, immediately forming an orange solution. After the mixture was stirred for 54 h, the resulting black solution was evaporated to a small volume (≈ 3 mL). The addition of diethyl ether (10 mL) gave **9** as a gray solid (0.131 g, 71% yield). After recrystallization in acetone/*n*-hexane complex **9** was obtained a light gray solid (0.08 g, 43% yield). Anal. Calcd for $\text{C}_{73}\text{F}_{13}\text{H}_{45}\text{O}_3\text{P}_3\text{PtS}\cdot 2\text{CH}_2\text{Cl}_2$ ($M_r = 1705.99$): C, 52.80; H, 2.84; S, 1.88. Found: C, 53.26; H, 2.99; S, 2.17. Λ_M : 114 $\Omega^{-1}\text{cm}^2\text{mol}^{-1}$. MS ES (+): m/z 1387 ($[\text{M} - \text{TfO}]^+$, 100%). IR (cm^{-1}): $\nu(\text{C}\equiv\text{C})$ 2174 s; $\nu(\text{C}_6\text{F}_5)_{\text{X-sens}}$ 781 m; $\nu(\text{C}_6\text{F}_5-\text{C})$ 991 m, 989 m; $\nu(\text{CF}_3\text{SO}_3)$ 1275 s, br, 1225 m, 1157 s, br, 1031 s. ^1H NMR (CDCl_3 , 20 °C, δ): 7.82–6.30 (m, 38H), 6.24 (d, $J = 7.5$ Hz, 2H). ^{19}F NMR (CDCl_3 , 20 °C, δ): -78.4 (s, 3F, CF_3), -116.7 [m, $^3J(\text{Pt}-\text{F}_o) = 199$ Hz, 2F_o], -133.6 [d, $J = 17.4$ Hz, 2F_o , $\text{C}-\text{C}_6\text{F}_5$], -150.0 (t, 1F_p , $\text{C}-\text{C}_6\text{F}_5$), -158.4 (t, 1F_p), -159.5 (m, br, 2F_m , $\text{C}-\text{C}_6\text{F}_5$), -162.0 (m, 2F_m). $^{31}\text{P}\{^1\text{H}\}$ NMR (CDCl_3 , 20 °C, δ): 48.3 [s, br, $^1J(\text{P}^2-\text{Pt}) = 2196$ Hz, P^2 trans to C_6F_5], 43.1 [dd, $^1J(\text{P}^3-\text{Pt}) = 2410$ Hz, $^2J(\text{P}^3-\text{P}^1)_{\text{trans}} = 364$ Hz, $^2J(\text{P}^3-\text{P}^2)_{\text{cis}} = 15.6$ Hz, P^3], -5.5 [dd, $^1J(\text{P}^1-\text{Pt}) = 2566$ Hz, $^2J(\text{P}^1-\text{P}^3)_{\text{trans}} = 364$ Hz, $^2J(\text{P}^1-\text{P}^2)_{\text{cis}} = 12.9$ Hz, P^1].

Reaction of $[\text{Rh}(\text{COD})(\text{PPh}_2\text{C}\equiv\text{CPh})_2](\text{ClO}_4)$, **2, with *cis*- $[\text{Pt}(\text{C}_6\text{F}_5)_2(\text{THF})_2]$.** *cis*- $[\text{Pt}(\text{C}_6\text{F}_5)_2(\text{THF})_2]$ (0.076 g, 0.113 mmol) was added to a stirred solution of $[\text{Rh}(\text{COD})(\text{PPh}_2\text{C}\equiv\text{CPh})_2](\text{ClO}_4)$, **2** (0.100 g, 0.113 mmol), in CH_2Cl_2 (15 mL) at 20 °C, immediately forming an orange solution. Monitoring the reaction by multinuclear NMR spectroscopy in CDCl_3 at room temperature revealed the presence after 10 min of several products containing $\text{C}-\text{C}_6\text{F}_5$ [δ_{F} -125.5, -131.3, -138.5, -141.4 (F_o), -152.9, -153.5, -158.1, -159.8 (F_p)], starting material (**2**), and *cis*- $[\text{Pt}(\text{C}_6\text{F}_5)_2(\text{PPh}_2\text{C}\equiv\text{CPh})_2]$. After 8 h of reaction, the same mixture was observed but in different proportions. Attempts to obtain a pure insertion product were unsuccessful.

Reaction of $[\text{Ir}(\text{COD})(\text{PPh}_2\text{C}\equiv\text{CPh})_2](\text{ClO}_4)$, **3, with *cis*- $[\text{Pt}(\text{C}_6\text{F}_5)_2(\text{THF})_2]$.** A mixture of *cis*- $[\text{Pt}(\text{C}_6\text{F}_5)_2(\text{THF})_2]$ (0.045 g, 0.067 mmol) and $[\text{Ir}(\text{COD})(\text{PPh}_2\text{C}\equiv\text{CPh})_2](\text{ClO}_4)$, **3** (0.065 g, 0.067 mmol), was dissolved at -40 °C in CH_2Cl_2 (15 mL), and the orange-brown solution obtained was layered with *n*-hexane. Cooling at -40 °C for 1 week afforded white crystals of $[(\text{C}_6\text{F}_5)_2\text{Pt}(\mu\text{-}\kappa\text{O}:\eta^2\text{-PPh}_2(\text{O})\text{C}\equiv\text{CPh})_2]$, **10**, and a dark-brown oil. NMR multinuclear study of this oil indicates the presence of a very impure insertion product together with an small amount of **3**. ^{19}F NMR (CDCl_3 , 20 °C, δ): -117 to -122 (br, F_o), -124.5 (F_o , $\text{C}-\text{C}_6\text{F}_5$), -132.2 (F_o , $\text{C}-\text{C}_6\text{F}_5$), -153.2 (F_p , $\text{C}-\text{C}_6\text{F}_5$), -159.5 to -166.5 (F_p , F_m). $^{31}\text{P}\{^1\text{H}\}$ NMR (CDCl_3 , 20 °C, δ): 40.9 [d, $J(\text{P}-\text{P}) = 18$ Hz], 27.9 [d, $J(\text{P}-\text{P}) = 18$ Hz]. Similar results were obtained by monitoring the reaction at room temperature.

Synthesis of $[(\text{C}_6\text{F}_5)_2\text{Pt}(\mu\text{-}\kappa\text{O}:\eta^2\text{-PPh}_2(\text{O})\text{C}\equiv\text{CPh})_2]$, **10.** To a solution of *cis*- $[\text{Pt}(\text{C}_6\text{F}_5)_2(\text{THF})_2]$ (0.150 g, 0.223 mmol) in CH_2Cl_2 was added 0.067 g (0.223 mmol) of $\text{PPh}_2(\text{O})\text{C}\equiv\text{CPh}$. After 5 min of stirring, a white solid precipitates. The solid was filtered out (0.15 g, 81% yield) Anal. Calcd for $\text{C}_{32}\text{F}_{10}\text{H}_{15}\text{OPPt}$: C, 46.22; H, 1.82. Found: C, 46.03; H, 1.90. IR (cm^{-1}): $\nu(\text{C}\equiv\text{C})$ 1981 s; $\nu(\text{P}-\text{O})$ 1165 s; $\nu(\text{C}_6\text{F}_5)_{\text{X-sens}}$ 815 s, 803 s.

Synthesis of $[\text{Pt}(\text{PPh}_2\text{C}\equiv\text{CPh})(\mu\text{-}\kappa\text{O}-o\text{-C}_6\text{H}_4\text{O}_2)(\mu\text{-}\kappa\text{P}:\eta^2\text{-PPh}_2\text{-C}\equiv\text{CPh})\text{Pt}(\text{C}_6\text{F}_5)_2]$, **11.** *cis*- $[\text{Pt}(\text{C}_6\text{F}_5)_2(\text{THF})_2]$ (0.094 g, 0.140 mmol) was added to an orange solution of $[\text{Pt}(o\text{-C}_6\text{H}_4\text{O}_2)(\text{PPh}_2\text{C}\equiv\text{CPh})_2]$ (**6**) (0.102 g, 0.116 mmol) in CH_2Cl_2 (20 mL), and the

mixture was stirred for 1 h. The solution was treated with charcoal and filtered through Kieselgurh. The yellow solution obtained was evaporated to small volume (2 mL) and treated with *n*-hexane (5 mL) to give **11** as a yellow-brown solid (0.149 g, 85% yield). Anal. Calcd for C₅₈F₁₀H₃₄O₂P₂Pt₂·CH₂Cl₂ (*M_r* = 1489.95): C, 47.56; H, 2.44. Found: C, 47.71; H, 2.31. MS ES (+): *m/z* 1405 ([M]⁺, 5%), 766 ([Pt(PPh₂C≡CPh)₂]⁺, 35%). IR (cm⁻¹): ν(C≡C) 2175 vs, 1968 s, br; ν(C₆F₅)_{Xsens} 802 vs, br. ¹H NMR (CDCl₃, 20 °C, δ): 8.12 (m, 3H), 7.94 (m, 4H), 7.60–7.12 (m, 20H), 7.03 (d, *J* = 7.4 Hz, 1H), 6.96 (d, *J* = 7.7 Hz, 1H), 6.74 (d, *J* = 7.5 Hz, 2H), 6.55 (d, 1H), 6.48 (t, 1H), 6.30 (t, 1H), (Ph, C₆H₄). ¹⁹F NMR (CDCl₃, 20 °C, δ): -118.7 [m, ³*J*(Pt–F_o) ~ 375 Hz, 3F_o], -119.1 [m, ³*J*(Pt–F_p) ~ 310 Hz, 1F_p], -161.5 (t, 1F_p), -162.5 (t, 1F_p), -163.8 (m, 1F_m), -164.9 (m, 1F_m), -165.6 (m, 2F_m). ³¹P{¹H} NMR (CDCl₃, 20 °C, δ): -2.7 [d, ¹*J*(Pt–P¹) = 3404 Hz, *J*(P¹–P²) = 27 Hz, P¹ bridge], -24.8 [d, ¹*J*(Pt–P²) = 4056 Hz, P² terminal].

Synthesis of [Pt(PPh₂C≡CPh)(μ-κS-o-C₆H₄S₂)(μ-κP:η²-PPh₂C≡CPh)Pt(C₆F₅)₂], **12.** This complex was obtained as a grayish product in a way similar to that for **11** but starting from [Pt(o-C₆H₄S₂)(PPh₂C≡CPh)₂] (**7**) (0.078 g, 0.086 mmol) and *cis*-[Pt(C₆F₅)₂(THF)₂] (0.058 g, 0.0865 mmol) (0.071 g, 57% yield). Anal. Calcd for C₅₈F₁₀H₃₄P₂Pt₂S₂·CH₂Cl₂ (*M_r* = 1522.07): C, 46.56; H, 2.38; S 4.21. Found: C, 46.32; H, 2.15; S 4.20. MS ES (+): *m/z* 933 ([Pt(C₆F₅)₂(PPh₂C≡CPh)₂] – H)⁺, 100%), 909 ([Pt(o-C₆H₄S₂)(PPh₂C≡CPh)₂] + H)⁺, 52%), 668 ([Pt(o-C₆H₄S₂)(C₆F₅)₂] – H)⁺, 39%). IR (cm⁻¹): ν(C≡C) 2174 vs, 1975 m, br; ν(C₆F₅)_{Xsens} 804 s, 793 s. ¹H NMR (CDCl₃, 20 °C, δ): 7.79 (m, 8H), 7.47–7.10 (m, 22H), 6.97 (d, *J* = 7.4 Hz, 2H) (Ph, C₆H₄), 6.79 (t, 1H), 6.65 (t, 1H) (C₆H₄). ¹⁹F NMR (CDCl₃, 20 °C, δ): -115.5 [m, br, ³*J*(Pt–F_o) ~ 415 Hz, 2F_o], -116.8 [dm, ³*J*(Pt–F_o) = 385 Hz, 2F_o], -162.0 (t, 1F_p), -163.3 (t, 1F_p), -164.4 (m, 2F_m), -164.9 (m, 2F_m). ³¹P{¹H} NMR (CDCl₃, 20 °C, δ): 5.0 [d, ¹*J*(Pt–P¹) = 2810 Hz, *J*(P¹–P²) = 29 Hz, P¹ bridge], -13.5 [d, ¹*J*(Pt–P²) = 3184 Hz, P² terminal].

Synthesis of [Pt(μ₃-κ²O, O'-o-C₆H₄O₂)(μ-κP:η²-PPh₂C≡CPh)₂]-[Pt(C₆F₅)₂]₂], **13.** To an orange solution of [Pt(o-C₆H₄O₂)(PPh₂C≡CPh)₂] (**6**) (0.102 g, 0.117 mmol) in CH₂Cl₂ (20 mL) was added *cis*-[Pt(C₆F₅)₂(THF)₂] (0.173 g, 0.257 mmol). The color of the resulting solution changed from orange to yellow-brown. The mixture was stirred for 2 h and then filtered through Kieselgurh. The filtrate was concentrated to small volume (2 mL) and treated with *n*-hexane (5 mL) to give **13** as a white solid (0.179 g, 80% yield). Anal. Calcd for C₇₀F₂₀H₃₄O₂P₂Pt₃ (*M_r* = 1934.26): C, 43.47; H, 1.77. Found: C, 43.68; H, 1.72. MS ES (+): *m/z* 766 ([Pt(PPh₂C≡CPh)₂]⁺, 30%), 875 ([**6**], 10%). IR (cm⁻¹): ν(C≡C) 1968 s, br; ν(C₆F₅)_{Xsens} 799 vs, br. ¹H NMR (CDCl₃, 20 °C, δ): 7.91 (d, br), 7.62–7.31 (m, 26H) Ph, 6.76 (s, br, 2H), 6.32 (s, br, 2H) C₆H₄. ¹⁹F NMR (CDCl₃, 20 °C, δ): -118.2 [m, ³*J*(Pt–F_o) ~ 425 Hz], -119.3 (m, br), 8F_o, -160.8 (br, 2F_p), -161.4 (t, 2F_p), -164.0 (m, br, 4F_m), -165.0 (m, 4F_m). ³¹P{¹H} NMR (CDCl₃, 20 °C, δ): -10.7 [s, ¹*J*(Pt–P) = 3813 Hz].

Synthesis of [Pt(μ₃-κ²S, S'-o-C₆H₄S₂)(μ-κP:η²-PPh₂C≡CPh)₂]-[Pt(C₆F₅)₂]₂], **14.** By a procedure similar to that described for **13**, [Pt(o-C₆H₄S₂)(PPh₂C≡CPh)₂] (**7**) (0.150 g, 0.165 mmol) and *cis*-[Pt(C₆F₅)₂(THF)₂] (0.250 g, 0.371 mmol) gave **14** as a brown solid (0.320 g, 93% yield). Anal. Calcd for C₇₀F₂₀H₃₄P₂Pt₃S₂ (*M_r* = 1966.35): C, 42.76; H, 1.74; S, 3.26. Found: C, 42.54; H, 1.63; S, 3.03. MS ES (+): *m/z* 933 ([Pt(C₆F₅)₂(PPh₂C≡CPh)₂] – H)⁺, 100%). IR (cm⁻¹): ν(C≡C) 1978 s, br; ν(C₆F₅)_{Xsens} 806 vs, 794 vs. ¹H NMR (CDCl₃, 20 °C, δ): 7.79 (d, *J* = 7.5 Hz, 6H), 7.53–7.25 (m, 24H) Ph, 7.14 (m, 2H), 6.85 (m, 2H) C₆H₄. ¹⁹F NMR (CDCl₃, 20 °C, δ): -115.8 [m, ³*J*(Pt–F_o) = 388 Hz, 4F_o], -117.8 [m, ³*J*(Pt–F_o) = 330 Hz, 4F_o], -161.1 (br, 2F_p), -162.1 (t, 2F_p),

-163.6 (m, br, 4F_m), -164.3 (m, 4F_m). ³¹P{¹H} NMR (CDCl₃, 20 °C, δ): -1.2 [s, ¹*J*(Pt–P) = 3117 Hz, ³*J*(Pt–P) = 43 Hz].

X-ray Crystallography. Table 1 reports details of the structural analyses for all complexes. Colorless (**1**, **9**, **10**) or yellow (**2**, **8**, **14**) crystals were obtained by slow diffusion of *n*-hexane into a dichloromethane (**1**, **10**, **9**, at room temperature), chloroform (**2**, at room temperature), tetrahydrofuran (**8**), or toluene (**14**) solution of each compound at -30 °C, while yellow crystals of **7**·acetone were obtained by leaving an acetone solution of this complex to evaporate at room temperature. For complexes **1**, **9**, and **10**, 1, 2, and 0.75 molecules of CH₂Cl₂ and for complex **8** 3 molecules of THF were found, respectively, in the asymmetric unit. Complex **7** crystallizes with one molecule of acetone. X-ray intensity data were collected with a Nonius κCCD area-detector diffractometer, using graphite-monochromated Mo Kα radiation. Images were processed using the DENZO and SCALEPACK suite of programs,⁵¹ carrying out the absorption correction at this point for complex **2**. For the rest of complexes, the absorption correction was performed using SORTAV,⁵² except for complex **9** for which an empirical absorption correction was done using XABS2.⁵³ All the structures were solved by Patterson and Fourier methods using the DIRDIF92 program⁵⁴ and refined by full-matrix least squares on *F*² with SHELXL-97.⁵⁵ All non-hydrogen atoms were assigned anisotropic displacement parameters, and all hydrogen atoms were constrained to idealized geometries fixing isotropic displacement parameters of 1.2 times the *U*_{iso} value of their attached carbon for the phenyl and methine hydrogens and 1.5 for the methyl groups. For **14**, one phenyl ring (C(3)–C(8)) was refined as an idealized aromatic ring, and for **1**·CH₂Cl₂, **8**·3C₄H₈O, and **10**·1.5CH₂Cl₂, one solvent molecule showed positional disorder and was modeled adequately. For complexes **1**·CH₂Cl₂, **8**·3C₄H₈O, **9**·2CH₂Cl₂, **10**·1.5CH₂Cl₂, and **14**, residual peaks bigger than 1 e Å⁻³ close to their respective platinum atoms have been observed but with no chemical meaning. For complex **10**, three peaks slightly bigger than 1 e Å⁻³ are also observed in the vicinity of the solvent.

Results and Discussion

Mononuclear Complexes. The synthesis of mononuclear complexes is shown in Scheme 1. The cationic tris-(phosphine)platinum complex [Pt(C₆F₅)(PPh₂C≡CPh)₃](CF₃SO₃), **1**, is isolated as a white solid by removing the chlorine ligands in [Pt(μ-Cl)(C₆F₅)(tht)]₂ (tht = tetrahydrothiophene) with AgCF₃SO₃ (2 equiv) and subsequent treatment with PPh₂C≡CPh (6 equiv) in acetone (Scheme 1, path i). Similarly, as shown in Scheme 1, path ii, the cationic rhodium and iridium derivatives [M(COD)(PPh₂C≡CPh)₂](ClO₄) (M = Rh, **2**, and Ir, **3**) are obtained as orange (**2**) or pink (**3**) solids from the cationic species [M(COD)(acetone)_x](ClO₄) (M = Rh, Ir), prepared in situ in acetone (see Experimental Section for details) with the alkynylphosphine PPh₂C≡CPh (4 equiv).

(51) Otwinowski, Z.; Minor, W. In *Methods in Enzymology*; Carter, C. V., Jr., Sweet, R. M., Eds.; Academic Press: New York, 1997; Vol. 276A, p 307.

(52) Blessing, R. H. *Acta Crystallogr.* **1995**, *A51*, 33.

(53) Parkin, S.; Moezzi, B.; Hope, H. *J. Appl. Crystallogr.* **1995**, *28*, 53.

(54) Beursken, P. T.; Beursken, G.; Bosman, W. P.; de Gelder, R.; García-Granda, S.; Gould, R. O.; Smith, J. M. M.; Smykalla, C. *The DIRDIF92 program system*; Technical Report of the Crystallography Laboratory, University of Nijmegen: Nijmegen, The Netherlands, 1992.

(55) Sheldrick, G. M. *SHELX-97, a program for the refinement of crystal structures*; University of Göttingen: Göttingen, Germany, 1997.

Table 1. Crystallographic Data for Compounds [Pt(C₆F₅)(PPh₂C≡CPh)₃](CF₃SO₃)·CH₂Cl₂, **1**·CH₂Cl₂; [Rh(COD)(PPh₂C≡CPh)₂](ClO₄), **2**; [Pt(*o*-C₆H₄S₂)(PPh₂C≡CPh)₂]·CH₃COCH₃, **7**·CH₃COCH₃; [Pt(C₆F₅)(OH₂)μ-{C(Ph)=C(PPh₂)C(PPh₂)C(PPh₂)=C(Ph)(C₆F₅)}Pt(C₆F₅)-(PPh₂C≡CPh)](CF₃SO₃)·3THF; **8**·3THF, [(C₆F₅)(PPh₂C≡CPh)Pt{C₁₀H₄-1-C₆F₅-4-Ph-2,3-κPP'(PPh₂)₂}] (CF₃SO₃)·2CH₂Cl₂, **9**·2CH₂Cl₂; [(C₆F₅)₂Pt(μ-κO:η²-PPh₂(O)C≡CPh)₂]·1.5CH₂Cl₂, **10**·1.5CH₂Cl₂; and [{Pt(μ-κS:S'-*o*-C₆H₄S₂)(μ-κP:η²-PPh₂C≡CPh)₂]Pt(C₆F₅)₂], **14**

	1 ·CH ₂ Cl ₂	2	7 ·CH ₃ COCH ₃	8 ·3THF
empirical formula	C ₆₈ H ₄₇ Cl ₂ F ₈ O ₃ P ₃ PtS	C ₄₈ H ₄₂ ClO ₄ P ₂ Rh	C ₄₉ H ₄₀ OP ₂ PtS ₂	C ₉₁ H ₆₉ F ₁₈ O ₇ P ₃ Pt ₂ S
<i>M_w</i>	1455.02	883.12	965.96	2131.61
<i>T</i> , K	173(1)	173(1)	223(1)	173(1)
λ(<i>Mo</i> Kα), Å	0.710 73	0.710 73	0.710 73	0.710 73
cryst system, space group	triclinic, <i>P</i> $\bar{1}$	monoclinic, <i>P2₁/c</i>	orthorhombic, <i>Pnca</i>	monoclinic, <i>P2₁/a</i>
cryst dimens, mm	0.6 × 0.4 × 0.3	0.35 × 0.25 × 0.10	0.35 × 0.2 × 0.2	0.3 × 0.25 × 0.075
<i>a</i> , Å;	12.4836(2);	9.76160(10);	10.64900(10);	15.66040(10);
α, deg	99.2020(10)	90	90	90
<i>b</i> , Å;	15.6758(3);	20.5301(3);	14.82700(10);	23.0236(2);
β, deg	98.6290(10)	99.9280(10)	90	94.44
<i>c</i> , Å;	16.1148(3);	20.6733(3);	26.8650(3);	23.3432(2);
γ, deg	92.353(2)	90	90	90
<i>V</i> , Å ³ ; <i>Z</i>	3070.85(10); 2	4081.02(9); 4	4241.79(7); 4	8391.38(12); 4
ρ _{calcd} , Mg/m ³	1.574	1.437	1.513	1.687
abs coeff, mm ⁻¹	2.556	0.607	3.518	3.509
<i>F</i> (000)	1448	1816	1928	4200
θ range for data collcn, deg	4.09–27.88	1.41–29.85	4.09–27.87	4.12–26.37
index ranges	−16 ≤ <i>h</i> ≤ 16, −20 ≤ <i>k</i> ≤ 20, −21 ≤ <i>l</i> ≤ 21	0 ≤ <i>h</i> ≤ 12, −26 ≤ <i>k</i> ≤ 0, −28 ≤ <i>l</i> ≤ 25	−13 ≤ <i>h</i> ≤ 14, −19 ≤ <i>k</i> ≤ 19, −33 ≤ <i>l</i> ≤ 35	−19 ≤ <i>h</i> ≤ 19, −28 ≤ <i>k</i> ≤ 28, −29 ≤ <i>l</i> ≤ 29
reflns colld	46 433	9681	65 350	103 763
refinement method	full-matrix least-squares on <i>F</i> ²	full-matrix least-squares on <i>F</i> ²	full-matrix least-squares on <i>F</i> ²	full-matrix least-squares on <i>F</i> ²
data/restraints/params	14 397/2/794	9681/0/505	5045/0/251	17 095/5/1051
GOF on <i>F</i> ² ^a	1.035	1.022	0.991	1.043
final <i>R</i> indices [<i>I</i> > 2σ(<i>I</i>) ^a]	<i>R</i> 1 = 0.0416, w <i>R</i> 2 = 0.1007	<i>R</i> 1 = 0.0404, w <i>R</i> 2 = 0.0839	<i>R</i> 1 = 0.0253, w <i>R</i> 2 = 0.0511	<i>R</i> 1 = 0.0454, w <i>R</i> 2 = 0.1078
<i>R</i> indices (all data) ^a	<i>R</i> 1 = 0.0511, w <i>R</i> 2 = 0.1059	<i>R</i> 1 = 0.0623, w <i>R</i> 2 = 0.0935	<i>R</i> 1 = 0.0432, w <i>R</i> 2 = 0.0574	<i>R</i> 1 = 0.0606, w <i>R</i> 2 = 0.1157
largest diff peak and hole, e [−] Å ^{−3}	1.734 and −2.025	0.784 and −0.656	0.868 and −0.697	4.790 and −2.304

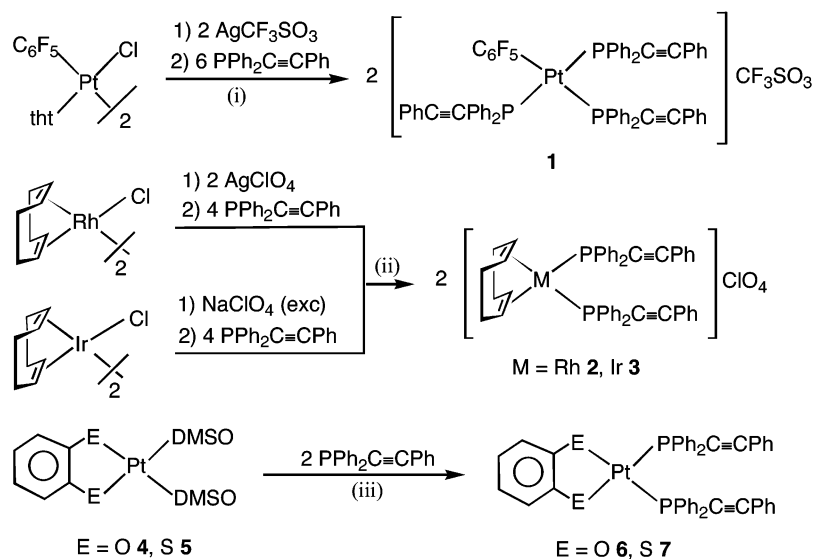
	9 ·2CH ₂ Cl ₂	10 ·1.5CH ₂ Cl ₂	14
empirical formula	C ₇₅ H ₄₈ Cl ₄ F ₁₃ O ₃ P ₃ PtS	C _{65.5} H ₃₃ Cl ₃ F ₂₀ O ₂ P ₂ Pt ₂	C ₇₀ H ₃₄ F ₂₀ P ₂ Pt ₃ S ₂
<i>M_w</i>	1705.99	1790.39	1966.30
<i>T</i> , K	173(1)	173(1)	223(1)
λ(<i>Mo</i> Kα), Å	0.710 73	0.710 73	0.710 73
cryst system, space group	monoclinic, <i>P2₁/c</i>	triclinic, <i>P</i> $\bar{1}$	triclinic, <i>P</i> $\bar{1}$
cryst dimens, mm	0.70 × 0.075 × 0.075	0.4 × 0.25 × 0.2	0.42 × 0.20 × 0.15
<i>a</i> , Å;	20.1780(3);	11.6299(2);	15.3996(3);
α, deg	90	102.8900(10)	107.1250(10)
<i>b</i> , Å;	15.3627(2);	12.1801(2);	15.7509(2);
β, deg	104.3490(10)	100.5700(10)	93.3460(10)
<i>c</i> , Å;	23.0999(3);	12.2589(2);	18.5369(4);
γ, deg	90	99.7760(10)	109.9680(10)
<i>V</i> , Å ³ ; <i>Z</i>	6937.32(16); 4	1623.30(5); 1	3974.89(13); 2
ρ _{calcd} , Mg/m ³	1.633	1.831	1.643
abs coeff, mm ⁻¹	2.360	4.579	5.441
<i>F</i> (000)	3384	859	1860
θ range for data collcn, deg	1.04–25.03	2.22–27.90	4.11–25.68
index ranges	−24 ≤ <i>h</i> ≤ 24, −18 ≤ <i>k</i> ≤ 18, −27 ≤ <i>l</i> ≤ 27	−15 ≤ <i>h</i> ≤ 15, −16 ≤ <i>k</i> ≤ 15, −16 ≤ <i>l</i> ≤ 16	−18 ≤ <i>h</i> ≤ 18, −19 ≤ <i>k</i> ≤ 19, −22 ≤ <i>l</i> ≤ 22
reflns colld	55 199	25 706	42 871
refinement method	full-matrix least-squares on <i>F</i> ²	full-matrix least-squares on <i>F</i> ²	full-matrix least-squares on <i>F</i> ²
data/restraints/params	12 146/0/901	7694/3/421	14 635/9/875
GOF on <i>F</i> ² ^a	1.049	1.055	1.054
final <i>R</i> indices [<i>I</i> > 2σ(<i>I</i>) ^a]	<i>R</i> 1 = 0.0520, w <i>R</i> 2 = 0.1490	<i>R</i> 1 = 0.0380, w <i>R</i> 2 = 0.0961	<i>R</i> 1 = 0.0428, w <i>R</i> 2 = 0.1134
<i>R</i> indices (all data) ^a	<i>R</i> 1 = 0.0801, w <i>R</i> 2 = 0.1822	<i>R</i> 1 = 0.0444, w <i>R</i> 2 = 0.0995	<i>R</i> 1 = 0.0580, w <i>R</i> 2 = 0.1252
largest diff peak and hole, e [−] Å ^{−3}	1.444 and −3.358	2.637 and −2.709	1.222 and −1.719

^a *R*1 = Σ(|*F_o*| − |*F_c*|)/Σ|*F_o*|; w*R*2 = [Σw(*F_o*² − *F_c*²)/Σw*F_o*²]^{1/2}; GOF = Σw(*F_o*² − *F_c*²)/(*N_{obs}* − *N_{param}*); w = [σ²(*F_o*) + (*g₁P*)² + *g₂P*]^{−1}; *P* = [max(*F_o*² + 2*F_c*²)/3].

Finally, the neutral platinum derivatives [Pt(*o*-C₆H₄E₂)-(PPh₂C≡CPh)₂] (*E* = O, **6**, and S, **7**) are synthesized as pale-orange (**6**) or gray (**7**) solids by displacing the dimethyl sulfoxide (DMSO) ligands from the neutral catecholate

[Pt(*o*-C₆H₄O₂)(DMSO)₂], **4**, or 1,2-benzenedithiolate [Pt(*o*-C₆H₄S₂)(DMSO)₂], **5**, complexes (also prepared in this work), with 2 equiv of the alkynylphosphine (Scheme 1, path iii). It should be mentioned that the synthesis of complex

Scheme 1

**Table 2.** Selected Bond Lengths (Å) and Angles (deg) for Complexes $[\text{Pt}(\text{C}_6\text{F}_5)(\text{PPh}_2\text{C}\equiv\text{CPh})_3](\text{CF}_3\text{SO}_3)_2 \cdot \text{CH}_2\text{Cl}_2$, **1**· CH_2Cl_2 ; $[\text{Rh}(\text{COD})(\text{PPh}_2\text{C}\equiv\text{CPh})_2](\text{ClO}_4)_2$, **2**; and $[\text{Pt}(\textit{o}\text{-C}_6\text{H}_4\text{S}_2)(\text{PPh}_2\text{C}\equiv\text{CPh})_2] \cdot \text{CH}_3\text{COCH}_3$, **7**· CH_3COCH_3

Complex 1 · CH_2Cl_2					
Pt(1)–C(61)	2.084(4)	P(3)–C(1)	1.744(4)	C(1)–C(2)	1.199(6)
Pt(1)–P(2)	2.3161(10)	P(2)–C(21)	1.747(4)	C(21)–C(22)	1.201(6)
Pt(1)–P(1)	2.3234(10)	P(1)–C(41)	1.750(4)	C(41)–C(42)	1.191(6)
Pt(1)–P(3)	2.3288(10)				
C(61)–Pt(1)–P(1)	88.75(11)	C(2)–C(1)–P(3)	173.3(4)	C(21)–C(22)–C(23)	179.3(5)
P(2)–Pt(1)–P(1)	92.21(4)	C(1)–C(2)–C(3)	178.0(5)	C(42)–C(41)–P(1)	172.3(4)
C(61)–Pt(1)–P(3)	86.68(11)	C(22)–C(21)–P(2)	174.8(4)	C(41)–C(42)–C(43)	179.4(5)
P(2)–Pt(1)–P(3)	92.26(4)				
Complex 2					
Rh(1)–C(44)	2.210(3)	Rh(1)–P(2)	2.2995(7)	P(2)–C(9)	1.673(3)
Rh(1)–C(41)	2.226(3)	Rh(1)–P(1)	2.3337(7)	C(1)–C(2)	1.168(4)
Rh(1)–C(42)	2.232(3)	P(1)–C(1)	1.694(3)	C(9)–C(10)	1.152(4)
Rh(1)–C(43)	2.262(3)				
C(41,42)–Rh(1)–P(2)	85.93	C(1)–P(1)–Rh(1)	115.39(11)	C(1)–C(2)–C(3)	175.2(3)
C(43,44)–Rh(1)–P(1)	84.23	C(9)–P(2)–Rh(1)	109.04(11)	C(10)–C(9)–P(2)	176.3(3)
P(2)–Rh(1)–P(1)	98.25(2)	C(2)–C(1)–P(1)	168.1(3)	C(9)–C(10)–C(11)	176.1(3)
Complex 7 · CH_3COCH_3					
Pt(1)–P(1)	2.2745(7)	P(1)–C(4)	1.759(3)	C(1)–C(1a)	1.393(7)
Pt(1)–S(1)	2.3052(7)	S(1)–C(1)	1.760(3)	C(4)–C(5)	1.199(4)
P(1a)–Pt(1)–P(1)	93.58(4)	C(1a)–C(1)–S(1)	121.37(11)	C(5)–C(4)–P(1)	172.5(3)
P(1)–Pt(1)–S(1)	88.84(3)	C(2)–C(1)–S(1)	119.7(3)	C(4)–C(5)–C(6)	177.0(3)
S(1)–Pt(1)–S(1a)	88.79(4)				

$[\text{Pt}(\textit{o}\text{-C}_6\text{H}_4\text{O}_2)(\text{PPh}_2\text{C}\equiv\text{CPh})_2]$, **6**, has been previously reported,²⁸ although in lower yield by reacting directly $[\text{PtCl}_2(\text{PPh}_2\text{C}\equiv\text{CPh})_2]$ in CHCl_3 with deprotonated catechol in MeOH . However, in our hands, this procedure yielded a complex mixture of products (with **6** being the major component) from which complex **6** can be separated after repeated crystallizations in very low yield. A solution of $[\text{Pt}(\textit{o}\text{-C}_6\text{H}_4\text{S}_2)(\text{PPh}_2\text{C}\equiv\text{CPh})_2]$, **7**, in acetone forms bright yellow crystals of $[\text{Pt}(\textit{o}\text{-C}_6\text{H}_4\text{S}_2)(\text{PPh}_2\text{C}\equiv\text{CPh})_2] \cdot \text{CH}_3\text{COCH}_3$ (**7**· CH_3COCH_3) suitable for X-ray diffraction. Despite the different color of both samples, the only significant difference between **7** and **7**· CH_3COCH_3 in their spectroscopic data is the presence of acetone.

All complexes are air-stable and have been characterized by the usual analytical and spectroscopic techniques. Additionally, the molecular structures of the cationic **1**, **2**, and neutral **7**· CH_3COCH_3 derivatives have been determined by

X-ray diffraction. The IR spectra of phosphine complexes show one $\nu(\text{C}\equiv\text{C})$ strong absorption in the $2171\text{--}2177\text{ cm}^{-1}$ region thus confirming the P-coordination mode of the $\text{PPh}_2\text{C}\equiv\text{CPh}$ ligand.^{2–6,15,40,41,43,56} The bis(alkynylphosphine) complexes (**2**, **3**, **6**, **7**) exhibit a singlet phosphorus resonance (range $\delta = 14.5$ to 8.25), downfield shifted with respect to that of free $\text{PPh}_2\text{C}\equiv\text{CPh}$ ($\delta = -33.55$), and as expected, the tris(alkynylphosphine) complex **1** shows a doublet at $\delta = -6.3$, attributed to the two phosphines mutually trans, and a signal at $\delta = -7.5$, assigned to the phosphine ligand trans to C_6F_5 , which appears as a multiplet due to additional unresolved coupling to fluorine atoms. The $^{13}\text{C}\{^1\text{H}\}$ NMR spectra are particularly significant. In all complexes, the C_α carbon resonances are shifted upfield ($\delta = 77.9\text{--}81.1$) with respect to that of free $\text{PPh}_2\text{C}\equiv\text{CPh}$ ($\delta(\text{C}_\alpha) = 86.5$), this effect being similar in cationic or neutral complexes. The acetylenic C_β carbon resonances lie very close to that of the free ligand

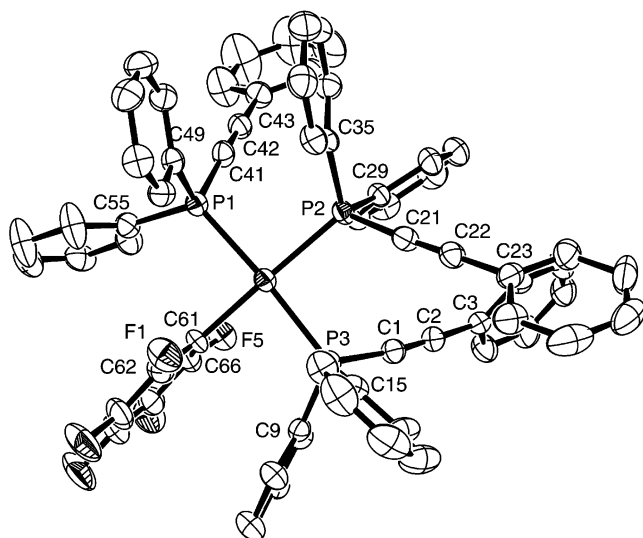


Figure 1. Molecular structure of the cation $[\text{Pt}(\text{C}_6\text{F}_5)(\text{PPh}_2\text{C}\equiv\text{CPh})_3]^+$ in $1\cdot\text{CH}_2\text{Cl}_2$. Ellipsoids are drawn at the 50% probability level. Hydrogen atoms are omitted for clarity.

($\delta(\text{C}_\beta)$ 109.4) but move slightly upfield in complex **1** and downfield in the rest of complexes. The resulting chemical shift difference [$\Delta(\delta(\text{C}_\beta) - \delta(\text{C}_\alpha))$], which can be related to the triple bond polarization,^{15,16,57} is similar in neutral Pt(II) (30, **6**; 26.6, **7**) or cationic [Rh(I), 28.3, or Ir(I), 28.6] complexes, being greatest in the cationic tris(phosphine) Pt(II) complex **1** (Δ 29.4 for $\text{C}\equiv\text{C}$ trans to C_6F_5 and 33.6 ppm for the equivalent $\text{C}\equiv\text{C}$ fragments cis to C_6F_5).

Although phosphinoalkyne mononuclear complexes of group 10 metals have been known for more than 30 years, very few of them have been structurally characterized.^{2,27,28,43} Details of the crystallographic determinations for **1**, **2**, and $7\cdot\text{CH}_3\text{COCH}_3$ are presented in Table 1, and selected bond distances and angles are given in Table 2. The metal centers in the cations **1**⁺ and **2**⁺ and in the neutral complex **7** (Figures 1–3) are located in slightly distorted square-planar environments with unexceptional bond lengths (M–C, M–P) and angles for this type of complex.^{58,59} The Pt–S distances [2.3052(7) Å] in **7** are within the range of those observed for other platinum(II) dithiolate phosphine complexes⁶⁰ but longer than those seen in typical platinum diimine dithiolate derivatives.^{61–66}

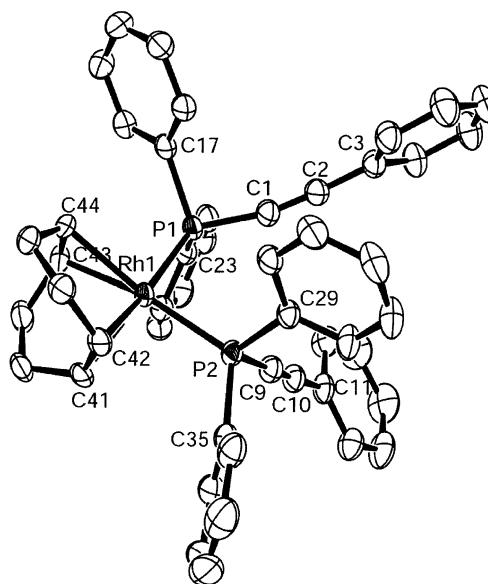


Figure 2. Molecular structure of the cation $[\text{Rh}(\text{COD})(\text{PPh}_2\text{C}\equiv\text{CPh})_2]^+$ in **2**. Ellipsoids are drawn at the 50% probability level. Hydrogen atoms are omitted for clarity.

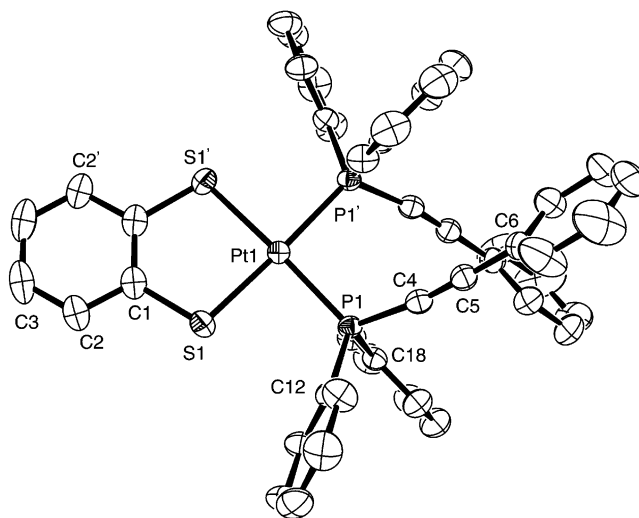
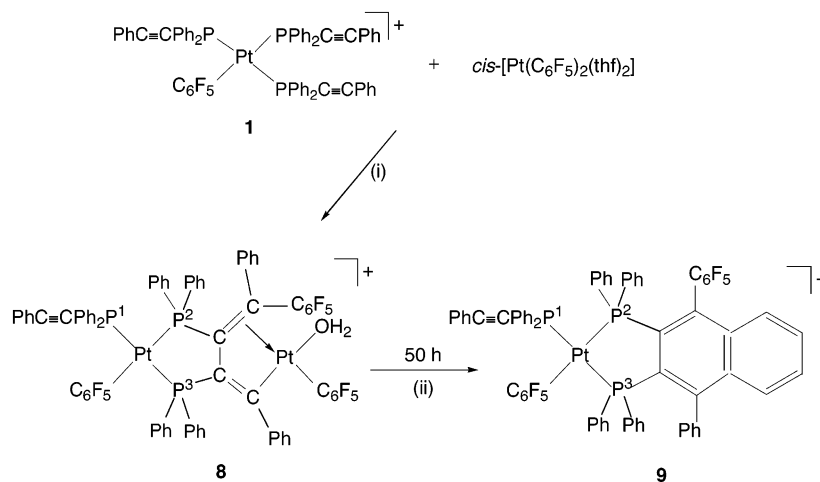


Figure 3. Molecular structure of $7\cdot\text{CH}_3\text{COCH}_3$. Ellipsoids are drawn at the 50% probability level. Hydrogen atoms are omitted for clarity.

The P–C(alkyne) and $\text{C}_\alpha\equiv\text{C}_\beta$ bond lengths are slightly shorter in the rhodium complex **2** [P– C_α 1.694(3), 1.673(3) Å; $\text{C}_\alpha\equiv\text{C}_\beta$ 1.168(4), 1.152(4) Å] than in the platinum derivatives **1** [1.744(4)–1.750(4) Å; 1.199(6)–1.201(6) Å] and **7** [1.759(3) Å; 1.199(4) Å]. The two *cis*-alkynyl entities in these complexes [P(3) and P(2) on **1**] are found staggered, with torsional angles $\text{C}_\alpha\text{--P--P'--C}_{\alpha'}$ of 68.6° [C(1)–P(3)–P(2)–C(21)] (**1**), 68.5° (**2**), and 66.3° (**7**) and dihedral angles between both P– $\text{C}_\alpha\text{--C}_\beta\text{--C}_\gamma$ fragments of 38.80° [P(3)–C(1)–C(2)–C(3) and P(2)–C(21)–C(22)–C(23)] (**1**), 56.83° (**2**), and 124.60° (**7**). The separation between the alkyne $\text{C}_\alpha\text{--C}_\alpha$ atoms [3.226 Å C(1)–C(21) (**1**), 3.403 Å (**2**), and 3.166 Å (**7**)] is in keeping with the distances observed in previous square-planar *cis*-bis(diphenyl)(alkynylphosphine)platinum(II) complexes, in which intramolecular coupling of phosphinoalkyne ligands was induced by heating^{27,28} or by metal complexation.^{42,43,67–69} As can be observed in Figure 1, in the cation **1**⁺, the mutually trans P(3) and P(1) P– $\text{C}\equiv\text{C}$ R

- (56) Forniés, J.; García, A.; Gómez, J.; Lalinde, E.; Moreno, M. T. *Organometallics* **2002**, *21*, 3733.
- (57) Louattani, E.; Lledós, A.; Suades, J.; Alvarez-Larena, A.; Piniella, J. F. *Organometallics* **1995**, *14*, 1053.
- (58) Ara, I.; Berenguer, J. R.; Eguizábal, E.; Forniés, J.; Lalinde, E.; Martínez, F. *Organometallics* **1999**, *18*, 4344.
- (59) Ara, I.; Berenguer, J. R.; Forniés, J.; Lalinde, E. *Organometallics* **1997**, *16*, 3921.
- (60) Bevilacqua, J. M.; Zuleta, J. A.; Eisenberg, R. *Inorg. Chem.* **1994**, *33*, 258.
- (61) Connick, W. B.; Gray, H. B. *J. Am. Chem. Soc.* **1997**, *119*, 11620.
- (62) Geary, E. A. M.; Hirata, N.; Clifford, J.; Durrant, J. R.; Parsons, S.; Dawson, A.; Yellowlees, L. J.; Robertson, N. *Dalton Trans.* **2003**, 3757.
- (63) Smucker, B. W.; Hudson, J. M.; Omary, M. A.; Dunbar, K. R. *Inorg. Chem.* **2003**, *42*, 4714.
- (64) Bevilacqua, J. M.; Eisenberg, R. *Inorg. Chem.* **1994**, *33*, 2913.
- (65) Keefer, C. E.; Bereman, R. D.; Purrington, S. T.; Knight, B. W.; Boyle, P. D. *Inorg. Chem.* **1999**, *38*, 2294.
- (66) Adams, C. J. *J. Chem. Soc., Dalton Trans.* **2002**, 1545.

Scheme 2



fragments are eclipsed and, curiously, this final disposition favors the presence of π -stacking interactions involving the C₆F₅ ligand and the C(9–14) and C(55–60) phenyl rings, the averages of the centroid–centroid distances being 3.495 and 3.905 Å, respectively. It has been previously noted that C₆H₅/C₆F₅ π interactions are attractive and a driving force in many crystallizations.⁷⁰

Reactions of Mononuclear Complexes with *cis*-[Pt(C₆F₅)₂(THF)₂]. With the aim of extending the insertion process described in the Introduction to other systems, we have examined the reactivity of the mononuclear P-coordinated alkynylphosphine complexes **1–3**, **6**, and **7** toward *cis*-[Pt(C₆F₅)₂(THF)₂]. As is shown in Schemes 2–4, the results depend on the mononuclear substrate employed. The cationic complex [Pt(C₆F₅)(PPh₂C≡CPh)₃](CF₃SO₃), **1**, reacts with 1 equiv of *cis*-[Pt(C₆F₅)₂(THF)₂] in CH₂Cl₂ at room temperature to immediately give an orange solution, from which the double inserted cationic product [Pt(C₆F₅)(S)- μ -{C(Ph)=C(PPh₂)C(PPh₂)=C(Ph)(C₆F₅)}Pt(C₆F₅)(PPh₂C≡CPh)](CF₃SO₃), **8**, is isolated as an orange solid in moderate yield (Scheme 2i). Although the solid-state crystal structure of crystals obtained by slow diffusion of *n*-hexane into a THF solution of **8** reveals that the complex crystallizes with 3 molecules of THF and that the vacant site created by the insertion process is occupied by a H₂O molecule, the bulk material and repeated elemental analysis was in keeping with the presence of 0.5 molecules of THF and 0.5 of H₂O. It should be noted that when the reaction is monitored by NMR spectroscopy at low temperature from –50 to –10 °C, no intermediates are detected and the product **8** is still not formed. The formation of inserted derivative **8** occurs initially at 0 °C, and at 20 °C the reaction is complete. The presence of the C–C₆F₅ unit is confirmed by IR (split bands at ~1500 and ~990 cm⁻¹)^{43,71,72} and ¹⁹F NMR spectroscopy. Thus, the

¹⁹F NMR spectrum confirms the presence of a static and typical organic C–C₆F₅ group, with the *ortho* (δ –122.1, –133.3) and *para* (–153.3) fluorine resonances up- and downfield shifted, respectively, relative to the resonances in *cis*-[Pt(C₆F₅)₂(THF)₂] (the *meta* fluorine resonances overlapped with the other F_{meta} signals). The rest of the spectrum is in agreement with the presence of two nonequivalent but free rotating C₆F₅ ligands. Furthermore, its ³¹P NMR spectrum exhibits the expected ABM spin system with Pt satellites. The low-frequency signal [dd, $J(\text{P}^1-\text{P}^3) = 362$, $J(\text{P}^1-\text{P}^2) = 14$ Hz], close to the value shown in the precursor (δ –5.9, **8**, vs –6.3, **1**), is assigned to the terminal PPh₂C≡CPh ligand (P¹). The most deshielded signal (δ 32.4), which appears as a broad singlet, due to long-range unresolved coupling to the F_o atoms of the mutually trans C₆F₅ group, and is flanked by one set of platinum satellites [$^1J(\text{Pt}-\text{P}^2) = 2214$ Hz], is assigned to phosphorus P² (trans to C₆F₅). The resonance at δ 28.2 appears as a doublet of doublets [$J(\text{P}^3-\text{P}^1) = 362$ Hz, $J(\text{P}^3-\text{P}^2) = 14.3$ Hz] and exhibits two sets of platinum satellites [$^1J(\text{P}^3-\text{Pt}) = 2428$ Hz, $^2J(\text{P}^3-\text{Pt}) = 530$ Hz] being therefore assigned to the phosphorus P³ mutually trans to P¹ and to the second Pt center. The ¹H NMR spectrum shows the presence of H₂O coordinated (δ 1.7 broad), which disappear after the addition of D₂O, and signals due to THF (3.71 s, br, OCH₂; 1.82 s, br, CH₂), suggesting that both solvents compete for the vacant coordination site. Crystals obtained by slow diffusion (–30 °C) of *n*-hexane into a THF solution of the complex were suitable for X-ray crystallography (Figure 4 and Tables 1 and 3). As can be seen, the 2,3-bis(diphenylphosphanyl)butadienyl ligand, formed by condensation of two of the three acetylenic fragments of the cationic complex **1** with one of the C₆F₅ groups of *cis*-[Pt(C₆F₅)₂(THF)₂], bridges the two platinum centers. The structural disposition is essentially similar to that previously described by us in the neutral complex [Pt(C₆F₅) μ -1 κ C¹(3,4) η :2 κ^2 PP'²{C(*t*Bu)=C(PPh₂)-C(PPh₂)=C(Tol)(C₆F₅)}Pt(C₆F₅)₂],⁴³ with the ligand display-

(67) Warner, B. P.; Millar, S. P.; Broene, R. D.; Buchwald, S. L. *Science* **1995**, *269*, 814.

(68) Coalter, N. L.; Concolino, T. E.; Streib, W. E.; Hughes, C. G.; Rheingold, A. L.; Zaleski, J. M. *J. Am. Chem. Soc.* **2000**, *122*, 3112.

(69) Schmitt, E. W.; Huffman, J. C.; Zaleski, J. M. *Chem. Commun.* **2001**, 167.

(70) Bauer, E. B.; Hampel, F.; Gladysz, J. A. *Organometallics* **2003**, *22*, 5567 and references given therein.

(71) Usón, R.; Forniés, J.; Espinet, P.; Lalinde, E.; Jones, P. G.; Sheldrick, G. M. *J. Chem. Soc., Dalton Trans.* **1982**, 2389.

(72) Usón, R.; Forniés, J.; Espinet, P.; Lalinde, E.; Jones, P. G.; Sheldrick, G. M. *J. Organomet. Chem.* **1983**, *253*, C47.

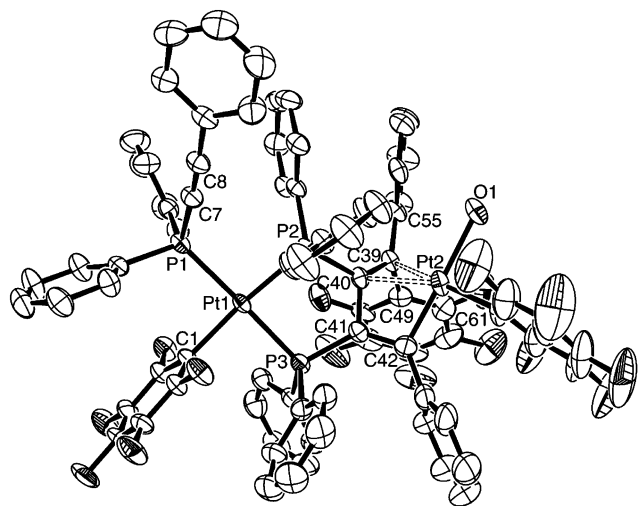


Figure 4. View of the molecular structure of the cation $[\text{Pt}(\text{C}_6\text{F}_5)(\text{OH}_2)\mu\{-\text{C}(\text{Ph})=\text{C}(\text{PPh}_2)\text{C}(\text{PPh}_2)=\text{C}(\text{Ph})(\text{C}_6\text{F}_5)\}\text{Pt}(\text{C}_6\text{F}_5)(\text{PPh}_2\text{C}\equiv\text{CPh})]^+$ in **8** showing the connectivity of the atoms.

Table 3. Selected Bond Lengths (Å) and Angles (deg) for $[\text{Pt}(\text{C}_6\text{F}_5)(\text{OH}_2)\mu\{-\text{C}(\text{Ph})=\text{C}(\text{PPh}_2)\text{C}(\text{PPh}_2)=\text{C}(\text{Ph})(\text{C}_6\text{F}_5)\}\text{Pt}(\text{C}_6\text{F}_5)(\text{PPh}_2\text{C}\equiv\text{CPh})](\text{CF}_3\text{SO}_3)\cdot 3\text{THF}$, **8**·3THF

Pt(1)–C(1)	2.080(5)	P(1)–C(7)	1.757(6)
Pt(1)–P(3)	2.3032(16)	P(2)–C(40)	1.850(6)
Pt(1)–P(2)	2.3189(13)	P(3)–C(41)	1.809(6)
Pt(1)–P(1)	2.3247(15)	C(7)–C(8)	1.190(8)
Pt(2)–C(42)	1.950(6)	C(39)–C(40)	1.434(8)
Pt(2)–C(61)	2.020(6)	C(39)–C(55)	1.490(8)
Pt(2)–O(1)	2.167(4)	C(39)–C(49)	1.520(8)
Pt(2)–C(40)	2.283(5)	C(40)–C(41)	1.487(8)
Pt(2)–C(39)	2.288(6)	C(41)–C(42)	1.372(9)
Pt(2)–C(41)	2.611(6)		
C(1)–Pt(1)–P(3)	89.02(16)	C(8)–C(7)–P(1)	176.1(6)
P(3)–Pt(1)–P(2)	87.07(5)	C(7)–C(8)–C(9)	176.4(7)
C(1)–Pt(1)–P(1)	89.48(16)	C(40)–C(39)–C(55)	126.8(5)
P(2)–Pt(1)–P(1)	94.34(5)	C(55)–C(39)–C(49)	112.1(5)
C(42)–Pt(2)–C(61)	95.6(3)	C(39)–C(40)–C(41)	117.4(5)
C(61)–Pt(2)–O(1)	85.7(3)	C(39)–C(40)–P(2)	131.1(5)
C(42)–Pt(2)–C(40)	65.3(2)	C(41)–C(40)–P(2)	109.3(4)
C(61)–Pt(2)–C(40)	155.4(2)	C(42)–C(41)–C(40)	107.0(5)
C(42)–Pt(2)–C(39)	84.4(2)	C(42)–C(41)–P(3)	131.8(5)
C(61)–Pt(2)–C(39)	163.7(3)	C(40)–C(41)–P(3)	120.4(4)
C(40)–Pt(2)–C(39)	36.56(19)	C(41)–C(42)–C(43)	127.4(6)
C(40)–Pt(2)–Pt(1)	106.20(18)	C(41)–C(42)–Pt(2)	102.2(4)
C(41)–P(3)–Pt(1)	105.4(2)	C(43)–C(42)–Pt(2)	130.3(5)

ing a $\mu\text{-}1\kappa\text{C}^1(3,4)\eta^2:2\kappa^2\text{PP}'$ bonding mode and acting as a vinylolefin ($\sigma\text{-}\eta^2$) ligand to the $\text{Pt}(2)(\text{C}_6\text{F}_5)(\text{H}_2\text{O})$ unit. Thus, Pt(2) coordinates to the C_{ipso} of the C_6F_5 group and the butadienyl backbone, which is σ -bonded through C(42) and η^2 -bonded through the C(39)–C(40) double bond. The vacant position, generated by the insertion process, is completed with a molecule of H_2O . The Pt–O distance [Pt–O 2.167(4) Å] is comparable to that found in the binuclear complex $[\text{Pt}_2(\text{H}_2\text{O})_2\text{Ph}_2(\text{ttab})](\text{BAR}_4)_2$ (ttab = 1,2,4,5-tetrakis(1-*N*-7-azaindolyl)benzene, Ar = 3,5-bis(trifluoromethyl)phenyl, 2.098(8) Å),⁷³ and the Pt–C(vinyl) bond length [Pt(2)–C(42) 1.950(6) Å] is rather short in agreement with the low trans influence of the oxygen donor ligand. The η^2 -olefin interaction [Pt(2)–C(39), C(40) 2.288(6), 2.283(5) Å] and the interatomic distances [C(39)–C(40) 1.434(8), C(40)–C(41) 1.487(8), C(41)–C(42) 1.372(9) Å] and angles about the

(73) Song, D.; Jia, W. L.; Wang, S. *Organometallics* **2004**, *23*, 1194.

butadienyl ligand [torsional angle C(42)–C(41)–C(40)–C(39) 60.1°] fall within the expected range.^{42,43} The dihedral angle between Pt(2)–C(39)–C(40) and Pt(2)–C(42)–C(61) is 58.13°. It is noteworthy that the olefinic C=C(C_6F_5)Ph fragment is located at the same side as the terminal alkynylphosphine, and this indicates that the reaction is again regioselective with the first insertion taking place in **1** with the $\text{PPh}_2\text{C}\equiv\text{CPh}$ ligand trans to the C_6F_5 group. Curiously, this acetylenic fragment exhibits the most shielded C_β resonance (δ 109.9 vs 111.5 in $\text{PPh}_2\text{C}\equiv\text{CPh}$ cis to C_6F_5) and also the least polarized alkyne fragment ($\text{M}-\text{PC}_\alpha^{\delta-}\equiv\text{C}_\beta^{\delta+}$ -Ph, $\Delta C_\beta-C_\alpha$ 29.4 vs 33.6). Another feature of the insertion process is that an overall stereoselective cis, cis diinsertion process has taken place, with the PPh_2 and Ph groups mutually cis in the vinyl unit and in the η^2 -alkene fragment. Both cis, trans⁷⁴ and cis, cis^{75–78} diinsertion acetylenic processes have been previously described. In our system, the final cis, cis stereoselectivity could be attributed to the simultaneous coordination of both phosphorus atoms to the cationic “ $\text{Pt}(\text{C}_6\text{F}_5)(\text{PPh}_2\text{C}\equiv\text{CPh})^+$ ” unit.

As is shown in Scheme 2ii, complex **8** is unstable giving on standing in CH_2Cl_2 solution at room temperature for ca. 50 h a very dark solution from which a novel cationic naphthalene-based diphenylphosphine mononuclear complex $[(\text{C}_6\text{F}_5)(\text{PPh}_2\text{C}\equiv\text{CPh})\text{Pt}\{\text{C}_{10}\text{H}_4\text{-}1\text{-C}_6\text{F}_5\text{-}4\text{-Ph-}2,3\text{-}\kappa\text{PP}'\text{-}(\text{PPh}_2)_2\}](\text{CF}_3\text{SO}_3)$, **9**, is isolated. The formation of the 1-pentafluorophenyl-2,3-bis(diphenylphosphine)-4-phenyl-naphthalene ligand has been previously observed by us in related neutral diinserted complexes.⁴³ As commented in the Introduction, mononuclear complexes containing the asymmetric naphthalene diphenylphosphine $[\text{C}_{10}\text{H}_5\text{-}1\text{-Ph-}2,3\text{-}\kappa\text{PP}'\text{-}(\text{PPh}_2)_2]$ have been also previously reported by Carty et al.^{27,28} However, the coupling reactions were only observed under very drastic conditions (reflux benzene). An easier coupling reaction (room temperature) has been recently found in a cyclic trimer of a neutral Pt–bis(alkynyl)diphosphine)-complex.² The ¹⁹F NMR spectrum of **9** confirms the presence of only two different sets of resonances, one of them corresponding to a C– C_6F_5 organic entity, and the ³¹P{¹H} NMR spectrum displays the expected ABM system with platinum satellites [$\delta(\text{P}^2)$ 48.3 (br), $\delta(\text{P}^3)$ 43.1 (dd), $\delta(\text{P}^1)$ –5.5 (dd), $J(\text{P}^1\text{-P}^3) = 364$ Hz]. However, from the NMR data it cannot be unambiguously determined whether the C– C_6F_5 group is in position 1 (syn to the terminal $\text{PPh}_2\text{C}\equiv\text{CPh}$ ligand) or in position 4 (anti to the $\text{PPh}_2\text{C}\equiv\text{CPh}$ ligand). It is immediately apparent from the X-ray diffraction study of **9** that the C– C_6F_5 and the terminal $\text{PPh}_2\text{C}\equiv\text{CPh}$ ligand are located mutually syn (Figure 5, Tables 1 and 4). The platinum center exhibits the expected square planar geometry with the phosphorus atoms [P(2), P(3)] of the formed 1-(pentafluorophenyl)-2,3-bis(diphenylphosphine)-4-phenyl-naphthalene ligand slightly displaced (0.016 and –0.022 Å)

(74) Pfeffer, M. *Pure Appl. Chem.* **1992**, *64*, 335.

(75) Yagyu, T.; Hamada, M.; Osakada, K.; Yamamoto, T. *Organometallics* **2001**, *20*, 1087 and references therein.

(76) Vicente, J.; Abad, J. A.; Fernández de Bobadilla, R.; Jones, P. G.; Ramírez de Arellano, M. C. *Organometallics* **1996**, *15*, 24.

(77) Maitlis, P. M. *J. Organomet. Chem.* **1980**, *200*, 161.

(78) Kelley, E. A.; Maitlis, P. M. *J. Chem. Soc., Dalton Trans.* **1979**, 167.

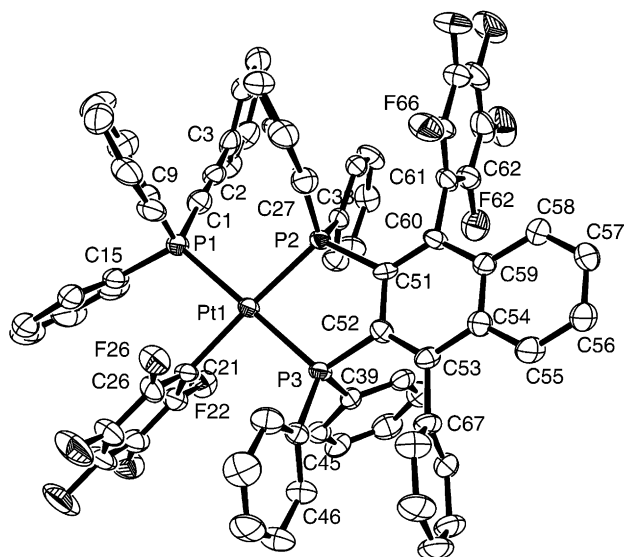


Figure 5. Molecular structure of the cation $[(C_6F_5)(PPh_2C\equiv CPh)Pt\{C_{10}H_4-1-C_6F_5-4-Ph-2,3-\kappa PP'(PPh_2)_2\}]^+$ in **9** with thermal ellipsoids at the 50% probability level. Hydrogen atoms are omitted for clarity.

from that plane. The bond lengths are in the expected range, and the slight deviation of the angles from a perfect square-planar geometry can be explained by steric effects of the chelating ligand. The naphthalene ring is also planar, and the dihedral angle with the platinum coordination plane is only 18.80° .

Attempts to stabilize analogous Rh–Pt or Ir–Pt insertion products were unsuccessful. Thus, NMR (^{31}P and ^{19}F) monitoring of the reaction of $[Rh(COD)(PPh_2C\equiv CPh)_2](ClO_4)$, **2**, with 1 equiv of cis - $[Pt(C_6F_5)_2(THF)_2]$ in $CDCl_3$ indicates the presence of a complex mixture, in which unknown insertion products ($C-C_6F_5$), cis - $[Pt(C_6F_5)_2(PPh_2C\equiv CPh)_2]$, and starting material (**2**) could be detected after 10 min and even 8 h of reaction. The formation of cis - $[Pt(C_6F_5)_2(PPh_2C\equiv CPh)_2]$ clearly indicates that the migration of phosphine ligands between electronically different metal centers competes with the insertion process. Unfortunately, the low stability of the insertion product precluded its isolation. On the other hand, when a mixture of cis - $[Pt(C_6F_5)_2(THF)_2]$ and $[Ir(COD)(PPh_2C\equiv CPh)_2](ClO_4)$, **3** (1:1 molar ratio), in CH_2Cl_2 at $-30^\circ C$ is layered with n -hexane and kept at $-30^\circ C$ for 1 week, white crystals of a new complex, characterized by X-ray crystallography as $[(C_6F_5)_2-$

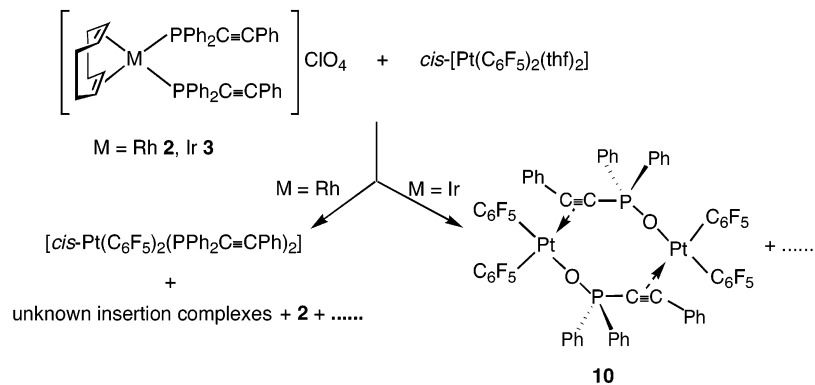
Table 4. Selected Bond Lengths (Å) and Angles (deg) for $[(C_6F_5)(PPh_2C\equiv CPh)Pt\{C_{10}H_4-1-C_6F_5-4-Ph-2,3-\kappa PP'(PPh_2)_2\}](CF_3SO_3)\cdot 2CH_2Cl_2$, **9**· $2CH_2Cl_2$

Pt(1)–C(21)	2.089(7)	C(51)–C(52)	1.432(9)
Pt(1)–P(3)	2.2905(19)	C(52)–C(53)	1.384(10)
Pt(1)–P(2)	2.2940(18)	C(53)–C(54)	1.433(10)
Pt(1)–P(1)	2.3333(19)	C(53)–C(67)	1.508(10)
P(2)–C(51)	1.861(7)	C(54)–C(59)	1.424(10)
P(3)–C(52)	1.829(7)	C(59)–C(60)	1.435(10)
C(1)–C(2)	1.193(10)	C(60)–C(61)	1.513(9)
C(51)–C(60)	1.369(10)		
C(21)–Pt(1)–P(3)	92.3(2)	C(51)–P(2)–Pt(1)	108.4(2)
P(3)–Pt(1)–P(2)	84.73(6)	C(52)–P(3)–Pt(1)	108.8(2)
C(21)–Pt(1)–P(1)	87.4(2)	C(52)–C(53)–C(67)	123.3(7)
P(2)–Pt(1)–P(1)	95.57(6)	C(51)–C(60)–C(61)	123.7(6)

$Pt(\mu\text{-}\kappa O:\eta^2\text{-}PPh_2(O)C\equiv CPh)_2$, **10**, are obtained together with a dark oil (Scheme 3). The NMR spectrum of the dark oil reveals the presence of a very impure inserted product (see Experimental Section for details). As was expected, complex **10** is alternatively obtained by reaction of cis - $[Pt(C_6F_5)_2(THF)_2]$ with 1 equiv of $PPh_2(O)C\equiv CPh$. The insolubility of this complex (**10**) precludes its characterization by NMR spectroscopy in solution. However, its IR spectrum reveals the presence of only one $\nu(C\equiv C)$ signal (1981 cm^{-1}) and the appearance of a new band in the $P=O$ stretching region (1165 cm^{-1}) at lower frequencies than those observed in $PPh_2(O)C\equiv CPh$ [$\nu(C\equiv C)$ $2173, 2156\text{ cm}^{-1}$; $\nu(P=O)$ 1194 cm^{-1}], in accordance with the presence of an acetylenic phosphine oxide coordinated through the oxygen atom and the acetylenic fragment.^{9,79,80}

As is shown in Figure 6 (see Tables 1 and 5), the two “ $Pt(C_6F_5)_2$ ” moieties in **10** are related by an inversion center and connected by two alkynylphosphine oxides ($Pt\cdots Pt$ 5.002 Å) which are coordinated acting as $1\kappa O:2\eta^2$ bridging ligands. In the resulting central eight-membered dimetallacycle, the atoms $C(1^a)-P(1)-O(1)$ and $C(1)-P(1^a)-O(1^a)$ are nearly coplanar [maximum deviation 0.099 Å , $P(1)$] with the platinum atoms [$Pt(1)$, $Pt(1^a)$] down and up (1.327 Å), respectively, from this plane. The η^2 -platinum–acetylenic linkage is asymmetric with the $Pt-C_\alpha$ distance [$2.167(4)\text{ Å}$] slightly shorter than the corresponding $Pt-C_\beta$ bond distance [$2.224(4)\text{ Å}$], and the $P-C_\alpha-C_\beta-C_\gamma$ skeleton shows a marked deviation from linearity [$P(1^a)-C(1)-C(2)$ $158.4(4)^\circ$, $C(1)-C(2)-C(3)$ $164.1(4)^\circ$]. The $P-C(1^a)$ [$1.763(5)\text{ Å}$] and the $P-O$ [$1.496(3)\text{ Å}$] bond lengths and the $O-P-C$

Scheme 3



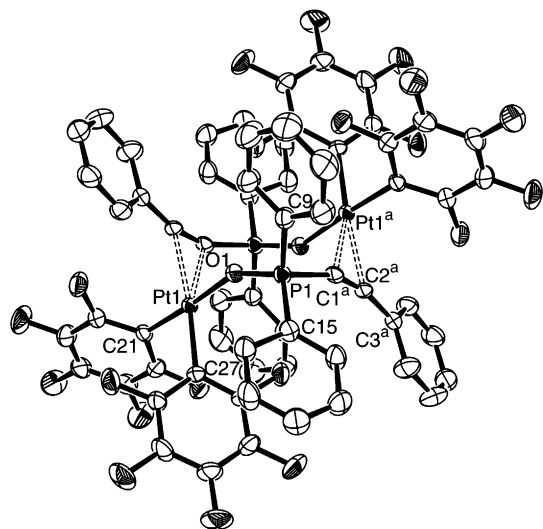


Figure 6. View of the molecular structure of the complex $[(\text{C}_6\text{F}_5)_2\text{Pt}(\mu\text{-}\kappa\text{O}:\eta^2\text{-PPh}_2(\text{O})\text{C}\equiv\text{CPh})]_2$, **10**, showing the atom-numbering scheme.

Table 5. Selected Bond Lengths (Å) and Angles (deg) for $[(\text{C}_6\text{F}_5)_2\text{Pt}(\mu\text{-}\kappa\text{O}:\eta^2\text{-PPh}_2(\text{O})\text{C}\equiv\text{CPh})]_2 \cdot 1.5\text{CH}_2\text{Cl}_2$, **10** · 1.5CH₂Cl₂

Pt(1)–C(21)	1.979(4)	P(1)–O(1)	1.496(3)
Pt(1)–C(27)	2.032(4)	P(1)–C(1 ^a)	1.763(5)
Pt(1)–O(1)	2.111(3)	C(1)–C(2)	1.238(6)
Pt(1)–C(1)	2.167(4)	C(2)–C(3)	1.434(6)
Pt(1)–C(2)	2.224(4)		
C(21)–Pt(1)–C(27)	88.28(18)	O(1)–P(1)–C(1 ^a)	111.4(2)
C(27)–Pt(1)–O(1)	91.96(15)	P(1)–O(1)–Pt(1)	148.9(2)
C(21)–Pt(1)–C(1)	92.75(17)	C(2)–C(1)–P(1 ^a)	158.4(4)
O(1)–Pt(1)–C(1)	88.86(15)	C(2)–C(1)–Pt(1)	76.2(3)
C(21)–Pt(1)–C(2)	96.22(17)	C(1)–C(2)–C(3)	164.1(4)
O(1)–Pt(1)–C(2)	82.40(14)	C(1)–C(2)–Pt(1)	71.1(3)

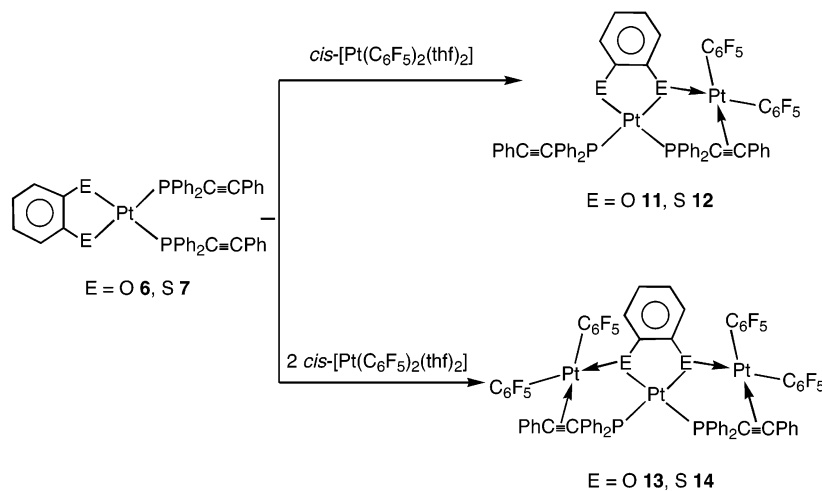
angle [111.4(2)°] are in the range of those observed in coordinated alkyne phosphine oxides.^{9,79,80}

The unexpected formation of an alkyne phosphine oxide complex starting from the corresponding alkyne phosphine ligand has been previously reported. For example, $[(\eta^5\text{-C}_5\text{H}_5)_2\text{Ni}_2(\text{PPh}_2(\text{O})\text{C}_2\text{CF}_3)]$, the first acetylenic phosphine oxide π complex structurally characterized, was obtained as one byproduct in the reaction of $[(\eta^5\text{-C}_5\text{H}_5)_2\text{Ni}]$ with $\text{PPh}_2\text{C}\equiv\text{CCF}_3$.⁷⁹ More recently, a cationic iron P-coordinated (diphenylphosphino)alkyne complex $[(\text{C}_5\text{H}_5)\text{Fe}(\text{CO})_2(\text{PPh}_2\text{C}\equiv\text{CPh})]$ -

(BF_4) was oxidized to an iron vinylidene phosphine oxide⁸¹ and the η^2 -alkynyl phosphine complex $[\text{Pt}(\eta^2\text{-PPh}_2\text{C}\equiv\text{CMe})\text{-}(\text{dcpe})]$ was oxidized in air to the corresponding phosphine oxide complex $[\text{Pt}\{\eta^2\text{-PPh}_2(\text{O})\text{C}\equiv\text{CMe}\}(\text{dcpe})]$.⁹

To check the possibilities of insertion in other systems, we have examined the reactions of the catecholate and dithiolate complexes **6** and **7** with *cis*- $[\text{Pt}(\text{C}_6\text{F}_5)_2(\text{THF})_2]$ in 1:1 and 1:2 molar ratios. However, the ability of these ligands (catecholate, dithiolate, and alkyne phosphine) to bridge metal atoms leads, in this case, to the formation of stable homo- bi- or trimetallic complexes containing mixed bridges $\mu\text{-}(o\text{-C}_6\text{H}_4\text{E}_2)/\mu\text{-PPh}_2\text{C}\equiv\text{CPh}$ systems (E = O, S) (Scheme 4). Reactions of $[\text{Pt}(o\text{-C}_6\text{H}_4\text{E}_2)(\text{PPh}_2\text{C}\equiv\text{CPh})_2]$ (E = O, **6**, and S, **7**) with 1 equiv of *cis*- $[\text{Pt}(\text{C}_6\text{F}_5)_2(\text{THF})_2]$ in CH₂Cl₂ yield bimetallic derivatives $[\text{Pt}(\text{PPh}_2\text{C}\equiv\text{CPh})(\mu\text{-}\kappa\text{E}\text{-}o\text{-C}_6\text{H}_4\text{E}_2)\text{-}(\mu\text{-}\kappa\text{P}:\eta^2\text{-PPh}_2\text{C}\equiv\text{CPh})\text{Pt}(\text{C}_6\text{F}_5)_2]$ (E = O, **11**, and S, **12**) as yellow-brown (**11**) or grayish (**12**) solids in high or moderate yields. Similar reactions with 2 equiv of *cis*- $[\text{Pt}(\text{C}_6\text{F}_5)_2(\text{THF})_2]$ afford the trimetallic complexes $\{[\text{Pt}(\mu_3\text{-}\kappa^2\text{EE}'\text{-}o\text{-C}_6\text{H}_4\text{E}_2)(\mu\text{-}\kappa\text{P}:\eta^2\text{-PPh}_2\text{C}\equiv\text{CPh})_2]\text{Pt}(\text{C}_6\text{F}_5)_2\}$ (E = O, **13**, and S, **14**) as a white **13** (80%) or brown **14** (93%) solid, respectively. The dimetallic or trimetallic formulation with the mixed heterobridged $(\mu\text{-}\kappa\text{E}\text{-}o\text{-C}_6\text{H}_4\text{E}_2)/(\mu\text{-}\kappa\text{P}:\eta^2\text{-PPh}_2\text{C}\equiv\text{CPh})$ or $(\mu_3\text{-}\kappa^2\text{EE}'\text{-}o\text{-C}_6\text{H}_4\text{E}_2)/(\mu\text{-}\kappa\text{P}:\eta^2\text{-PPh}_2\text{C}\equiv\text{CPh})_2$ systems has been established by elemental analysis and spectroscopic data and confirmed by an X-ray diffraction study on complex **14**. The presence of terminal and bridging alkyne phosphine groups in these complexes is inferred from the IR and NMR data. The binuclear complexes (**11**, **12**) display one broad $\nu(\text{C}\equiv\text{C})$ absorption, corresponding to the bridging ligand (1968 cm⁻¹, **11**; 1975 cm⁻¹, **12**), and another sharp one due to the terminal ligand (2175 cm⁻¹, **11**; 2174 cm⁻¹, **12**). By contrast, the trimetallic complexes **13** and **14** contain only one $\nu(\text{C}\equiv\text{C})$ broad band in the characteristic region of $\kappa\text{P}:\eta^2$ bridging $\text{PPh}_2\text{C}\equiv\text{CR}$ ligands (1968 cm⁻¹, **13**; 1978 cm⁻¹, **14**). Two different phosphorus resonances (AX systems) are seen in the ³¹P{¹H} NMR spectra of the binuclear complexes, confirming the inequivalence of both $\text{PPh}_2\text{C}\equiv\text{CPh}$ ligands. The low-field resonance (δ -2.7, **11**, and 5.0, **12**), significantly deshielded in relation to the

Scheme 4



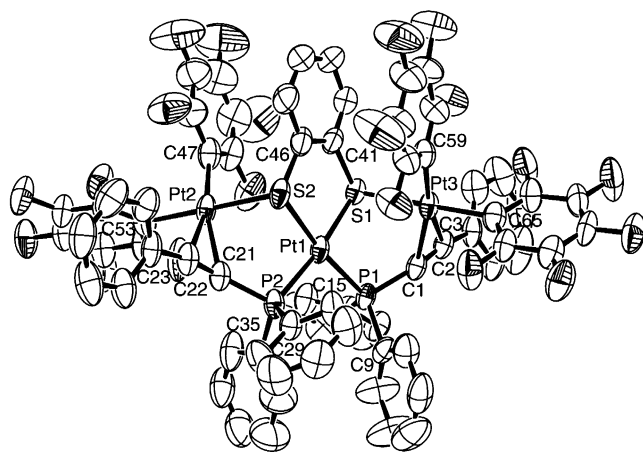


Figure 7. Molecular structure of $[\{\text{Pt}(\mu_3\text{-}\kappa^2\text{S},\text{S}'\text{-}o\text{-C}_6\text{H}_4\text{S}_2)(\mu\text{-}\kappa\text{P}:\eta^2\text{-PPh}_2\text{C}\equiv\text{CPh})_2\}\{\text{Pt}(\text{C}_6\text{F}_5)_2\}_2]$, **14**, showing the atom-numbering scheme.

corresponding precursors (δ -14.5 , **6**, and -4.7 , **7**), is attributed to the P atom of the bridging $\mu\text{-}\kappa\text{P}:\eta^2\text{-PPh}_2\text{C}\equiv\text{CPh}$, and the high-field signal (δ -24.8 , **11**, and -13.5 , **12**) is, therefore, assigned to the terminal P-coordinated ligand. As expected, a singlet phosphorus resonance ($\delta(\text{P})$ -10.7 , **13**, and -1.2 , **14**) with ^{195}Pt satellites is observed in the trinuclear complexes (**13**, **14**). In agreement with the formulations shown in Scheme 4, the ^{19}F NMR spectra reveal the presence of two nonequivalent and freely rotating C_6F_5 groups (AA'MXX' systems trans to $\text{C}\equiv\text{C}$ and trans to S) except complex **11** in which one of the rings is rigid on the NMR time scale (see Experimental Section for details). The aromatic protons of $\text{C}_6\text{H}_4\text{E}_2$ groups are seen as two symmetric multiplets in **13** and **14** (δ 6.76/6.32, **13**, and 7.14/6.85, **14**), while the more asymmetric binuclear complexes **11** and **12** give rise to one doublet (2H) and two triplets (1:1 H:H).

The structure of **14** is shown in Figure 7 (relevant data are summarized in Tables 1 and 6). In this complex, the bis-[(diphenylphenylethynyl)phosphine] precursor **7** acts as mixed bis(thiolate/ η^2 -alkyne) tetradentate ligand toward two "cis-Pt(C_6F_5) $_2$ " fragments in a such way that the thiolate ligand exhibits a simultaneous chelating and bridging bonding mode. The two sulfur atoms are chelating the Pt(1) atom and bridging the Pt(2) and Pt(3) centers, resulting in an homotrimeric Pt $_3$ assembly with the thiolate ligand coordinated to the three platinum atoms in $\mu_3\text{-}\kappa\text{SS}'$ form. Very few structural examples containing a benzenedithiolate ligand acting as $\mu_3\text{-}\kappa\text{SS}'$ bridging are presently known.^{82–90} To our knowledge, this complex (**14**) represents the first trimetallic

Table 6. Selected Bond Lengths (Å) and Angles (deg) for $[\{\text{Pt}(\mu_3\text{-}\kappa^2\text{S},\text{S}'\text{-}o\text{-C}_6\text{H}_4\text{S}_2)(\mu\text{-}\kappa\text{P}:\eta^2\text{-PPh}_2\text{C}\equiv\text{CPh})_2\}\{\text{Pt}(\text{C}_6\text{F}_5)_2\}_2]$, **14**

Pt(1)–P(2)	2.2799(19)	Pt(3)–C(1)	2.208(7)
Pt(1)–P(1)	2.2853(16)	Pt(3)–C(2)	2.242(6)
Pt(1)–S(1)	2.3237(18)	Pt(3)–S(1)	2.3864(16)
Pt(1)–S(2)	2.3307(16)	S(1)–C(41)	1.772(7)
Pt(2)–C(47)	2.042(9)	S(2)–C(46)	1.762(9)
Pt(2)–C(53)	2.044(7)	P(1)–C(1)	1.772(7)
Pt(2)–C(21)	2.198(7)	P(2)–C(21)	1.768(7)
Pt(2)–C(22)	2.250(7)	C(1)–C(2)	1.234(10)
Pt(2)–S(2)	2.3854(17)	C(21)–C(22)	1.238(9)
Pt(3)–C(59)	2.031(7)	C(41)–C(46)	1.401(11)
Pt(3)–C(65)	2.052(7)		
P(2)–Pt(1)–P(1)	98.88(7)	C(2)–Pt(3)–S(1)	88.41(17)
P(1)–Pt(1)–S(1)	86.25(6)	C(41)–S(1)–Pt(1)	104.9(3)
P(2)–Pt(1)–S(2)	87.19(7)	C(41)–S(1)–Pt(3)	110.0(2)
S(1)–Pt(1)–S(2)	88.24(7)	Pt(1)–S(1)–Pt(3)	94.56(6)
C(47)–Pt(2)–C(53)	86.4(3)	C(46)–S(2)–Pt(1)	104.1(3)
C(53)–Pt(2)–C(21)	101.6(3)	C(46)–S(2)–Pt(2)	110.0(3)
C(53)–Pt(2)–C(22)	90.3(3)	Pt(1)–S(2)–Pt(2)	96.76(6)
C(47)–Pt(2)–S(2)	93.1(2)	C(2)–C(1)–P(1)	156.2(6)
C(21)–Pt(2)–S(2)	78.88(18)	C(1)–C(2)–C(3)	162.0(7)
C(22)–Pt(2)–S(2)	90.17(18)	C(22)–C(21)–P(2)	153.3(6)
C(59)–Pt(3)–C(65)	86.4(3)	C(21)–C(22)–C(23)	164.5(8)
C(65)–Pt(3)–C(1)	102.1(3)	C(42)–C(41)–S(1)	120.2(6)
C(65)–Pt(3)–C(2)	91.1(3)	C(46)–C(41)–S(1)	120.2(6)
C(59)–Pt(3)–S(1)	93.7(2)	C(41)–C(46)–S(2)	122.4(6)
C(1)–Pt(3)–S(1)	78.15(17)	C(45)–C(46)–S(2)	119.3(7)

compound in which three metals are linked together by two mixed thiolate/ η^2 -alkynylphosphine bridging systems. The dihedral angles between the best square plane around each platinum center are Pt(1) plane–Pt(2) plane 75.72° , Pt(1) plane–Pt(3) 79.07° , and Pt(2) plane–Pt(3) 75.05° . The μ_3 -bridging thiolate ligand is nearly planar [dihedral angle between Pt(1)–S $_2$ and S $_2$ C $_6$ H $_4$ planes is $2.67(0.18)^\circ$] and adopts an anti conformation, with the platinum atoms, Pt(3) and Pt(2), located down (-2.0620 Å) and up (2.0057 Å) the Pt(1) coordination plane. The sulfur–platinum bond lengths are, as expected, slightly greater than that seen in **7**. The Pt(2,3)–C(acetylenic) bond distances [$2.198(7)$ – $2.250(7)$ Å] and the distortion from linearity of the acetylenic fragments are within the expected range. The platinum–platinum distances exclude any bonding interactions [Pt(1)–Pt(3) 3.461 Å and Pt(2)–Pt(1) 3.526 Å].

The cyclic voltammetric behavior of the catecholate and dithiolate complexes (**6**, **7**, **11**–**14**) has been examined, and the results are summarized in Table 7. The mononuclear complexes **6** and **7** exhibit two oxidation one-electron-transfer waves, which, with reference to previous studies,^{91–94} are tentatively attributed to ligand-based successive oxidations of the aromatic dianions (L^{2-}) to the semiquinone radical anions ($\text{L}^{\bullet-}$) and further to the quinones (L^0). For the catecholate mononuclear complex **6**, the first oxidation wave is reversible ($\Delta E = 222$ mV, $i_c/i_a = 1.10$) while the second peak at 0.94 V is irreversible. The dithiolate derivative **7** only gives two irreversible oxidation waves (0.46 and

(79) Restivo, R. J.; Fergusson, G.; Ng, T. W.; Carty, A. J. *Inorg. Chem.* **1977**, *16*, 172.

(80) Carty, A. J.; Paik, H. N.; Ng, T. W. *J. Organomet. Chem.* **1974**, *74*, 279.

(81) Louattani, E.; Moldes, I.; Suades, J. *Organometallics* **1998**, *17*, 3394.

(82) Chen, Y.-D.; Quin, Y.-H.; Zhang, L.-Y.; Shi, L.-X.; Chem, Z.-N. *Inorg. Chem.* **2004**, *43*, 1197.

(83) del Río, I.; Terroba, R.; Cerrada, E.; Hursthouse, M. B.; Laguna, M.; Light, M. E.; Ruiz, A. *Eur. J. Inorg. Chem.* **2001**, 2013.

(84) Cha, M.; Sletten, J.; Critchlow, S.; Kovacs, J. A. *Inorg. Chim. Acta* **1997**, *263*, 153.

(85) Gimeno, M. C.; Jones, P. G.; Laguna, A.; Laguna, M.; Terroba, R. *Inorg. Chem.* **1994**, *33*, 3932.

(86) Davila, R. M.; Elduque, A.; Grant, T.; Staples, R. J.; Fackler, J. P., Jr. *Inorg. Chem.* **1993**, *32*, 1749.

(87) Spence, M. A.; Rosair, G. M.; Lindsell, W. E. *J. Chem. Soc., Dalton Trans.* **1998**, 1581.

(88) Kang, B.; Peng, J.; Hong, M.; Wu, D.; Chen, X.; Weng, L.; Lei, X.; Liu, H. *J. Chem. Soc., Dalton Trans.* **1991**, 2897.

(89) Ehlich, H.; Schier, A.; Schmidbaur, H. *Organometallics* **2002**, *21*, 2400.

(90) Nakamoto, M.; Schier, A.; Schmidbaur, H. *J. Chem. Soc., Dalton Trans.* **1993**, 1347.

Table 7. Electrochemical Data^a (V) for Catecholate and Dithiolate Complexes **6**, **7**, and **11–14**

compd	E_{pa}^1	E_{pa}^2
6	-0.06 ^b (r)	0.94 (irr)
7	0.46 (irr)	0.97 (irr)
11	0.39 (qirr)	0.94 (irr)
12	0.36 (irr)	0.83 (irr)
13	0.28 (irr)	0.94 (irr)
14	—	—

^a Measured in CH₂Cl₂ (0.1 M (NBu₄)(PF₆) vs Fc/Fc⁺ at 20 °C and a scan rate of 200 mV s⁻¹). r = reversible, irr = irreversible, and qirr = quasiirreversible. ^b $E_{1/2}$ of reversible process.

0.97 V). The binuclear and trinuclear catecholate derivatives **11** and **13** also exhibit two anodic responses. The first anodic peak in **11** is quasiirreversible while the remaining responses are only poorly defined irreversible patterns. In both complexes, the first wave is anodically shifted (Δ 0.45 V, **11**, and 0.34 V, **13**) compared to the precursor which is consistent with the relative electron deficiency of the bridging catecholate ligand upon coordination to the “Pt(C₆F₅)₂” units. In contrast to this behavior, the trinuclear dithiolate complex does not give any anodic response and the binuclear derivative **12** shows a small feature at 0.36 V followed by a clear one-electron oxidation irreversible wave centered at 0.83 V.

Conclusions

In summary, we report the synthesis and structural characterization of several cationic or neutral mononuclear d⁸ (Pt, Rh, Ir) P-coordinated alkynylphosphine complexes **1–3**, **6**, and **7**. In these complexes, the ¹³C NMR studies suggest that the alkyne polarization upon alkyne complexation of PPh₂C≡CPh molecules is similar in neutral [Pt(II)] or cationic [Rh(I), Ir(I)] derivatives. The reactivity pattern

of these compounds toward the labile solvento species *cis*-[Pt(C₆F₅)₂(THF)₂] is strongly influenced by the metal, the charge, and the ligands. Starting from the cationic tris-(phosphine)platinum complex **1**, its reaction with “*cis*-Pt-(C₆F₅)₂” induced a regio- and stereoselective *cis*, *cis*-diinsertion process yielding the binuclear σ,π -butadienyl-diphosphine bridging complex (**8**) in which the resulting Pt-(σ,π -butadienyl)(C₆F₅) fragment is stabilized by a solvent donor molecule (THF, H₂O). This complex **8** is unstable in solution decomposing with loss of a PtC₆F₅ fragment and yielding a naphthalene-based diphenylphosphine mononuclear complex **9**. However, attempts to stabilize related cationic heterobinuclear Rh/Pt or Ir/Pt products were unsuccessful primarily due to low stability of the resulting products and the existence of competing phosphine exchange processes. Using the iridium complex **3** as precursor we were only able to isolate the alkynylphosphine oxide diplatinum complex **10**. By contrast, the catecholate (**6**) or 1,2-benzenedithiolate (**7**) derivatives, which contain additional potential bridging donor atoms (O, S), react with the *cis*-[Pt(C₆F₅)₂(THF)₂] complex yielding novel and unprecedented heterobridged (μ - κE -*o*-C₆H₄E₂)/(μ - κP : η^2 -PPh₂C≡CPh) binuclear complexes **11** and **12** or (μ - $\kappa^2 EE'$ -*o*-C₆H₄E₂)/(μ - κP : η^2 -PPh₂C≡CPh)₂ trinuclear species **13** and **14**. The formation of complexes **11** and **12** indicates that the η^2 -bonding capability of PPh₂C≡CPh competes efficiently with the donor ability of the O or S atoms, since more symmetric binuclear species with both oxygen or sulfur acting as bridging centers could have been formed.

Acknowledgment. This work was supported by the Spanish Ministerio de Ciencia y Tecnología (Project BQU2002-03997-C02-01, 02) and the Government of La Rioja (ACPI-2002/08). A.G. wishes to thank the MCYT for a grant, and M.B. thanks the Government of La Rioja for a grant.

Supporting Information Available: Crystallographic data in CIF format. This material is available free of charge via the Internet at <http://pubs.acs.org>.

IC048987J

- (91) Ghosh, P.; Begum, A.; Herebian, D.; Bothe, E.; Hildenbrand, K.; Weyhermüller, T.; Wieghardt, K. *Angew. Chem., Int. Ed.* **2003**, *42*, 563.
 (92) Cocker, T. M.; Bachman, R. E. *Inorg. Chem.* **2001**, *40*, 1550.
 (93) Pal, S.; Das, D.; Sinha, C.; Kennard, C. H. L. *Inorg. Chim. Acta* **2001**, *313*, 21.
 (94) Rauth, G. K.; Pal, S.; Das, D.; Sinha, C.; Slawin, A. M. Z.; Woollins, J. D. *Polyhedron* **2001**, *20*, 363.